Extended Project Qualification

How do physical changes in the environment affect the iridescence of a beetle?

By Elsa Lawrence
Tutor: Dr Parker

Contents:

1. Common biological/physical definitions and glossary:

- Chitin- a translucent, polysaccharide (derivative of glucose) that is found in many cell walls and exoskeletons of animals and insects. It has a function similar to that of the protein keratin.
- Critical angle- the angle of incidence beyond which rays totally internally reflect instead of refracting, along a more optically dense to a less optically dense medium boundary.
- Elytron (plural: elytra)- the protective wing-casing of certain insect orders, particularly beetles.
- Exoskeleton/integument- the external skeleton that supports and protects an animal's body.
- Iridescence- the property of some materials that appear to change colour when it is viewed from different angles.
- Optical thickness/refractive index- a value for the ratio between the speed of light in a vacuum and the speed of light through that material.
- Path difference- the amount by which the path travelled by one wave is longer than the path travelled by the other wave.
- Phase difference- the amount by which one wave lags behind another.
- Reflection- when a wave deflects back after hitting a boundary.
- Refraction- when the wave changes direction (as a result of slowing down or speeding up) as it enters a different medium.
- Sclerotisation- hardening of the exoskeleton.
- Total internal reflection/absolute reflection- when a wave/ray deflects completely along a more optically dense to a less optically dense medium boundary, when the critical angle is exceeded.

2. Abstract:

A material can be labelled ‘iridescent’ if the wavelength of the light reflected from it varies as the angle of viewing is changed. The species of beetles investigated were the *Chrysochroa wallacei, Chrysochroa rajah, Chrysochroa fulgidissima* and *Torynorrhina flammea flammea.* Beetles of the first three species are long and thin, perhaps as a result of belonging to the same genus, and are coloured mainly green/blue from all angles of viewing. However, the *T. flammea flammea* is shorter and wider and has a more red-tinted outer shell as well as a red stripe down the centre of each elytron (wing case/exoskeleton of each wing).
Light produced by a Halogen light source was shone on the elytra of the beetles and a Spatial Spectrophotometer measured the light intensity and wavelength of the reflected light. Then, a graph of wavelength against light intensity of the light reflected from the wing surface was produced by SpectraSuite. These beetles exhibit iridescent properties because as the angle of incidence increased, the peak wavelength gradually shifted towards the left; the wavelength of structural colour reflected decreased. In addition, to make sure that this shift was due to structure and not pigment, red and green card was tested. In contrast to the beetle wings, the peak wavelength for these tests did not shift as the angle increased, confirming that the card is not iridescent.
Furthermore, the *C. wallacei* and *T. flammea flammea* were tested to see if their iridescent colours change due to environmental changes such as high temperatures and dehydration. The first set of results for the heat treated *C. wallacei* were obtained by keeping the angle constant at which the graphs of wavelength against intensity were recorded, along with the temperature recorded every 30 seconds, and repeating this procedure for 6 different incident angles. The second set include the graphs obtained when the angle was not kept constant; as the wing case was cooling down the graphs were collected over a range of incident angles. The first set of results of the heated *C. wallacei* show that at the specific angles tested, the wavelength of light reflected decreases after

heat treatment and increases as the wing cools down. However, the second set show that the wavelength still decreases as the angle of incidence increases over a range of temperatures, showing that it still exhibits iridescence. Also, for the NaOH (sodium hydroxide) treated *C. wallacei* results, the wavelength decreases as the angle of incidence increases, again showing that the elytra is still iridescent, but overall the wavelength increases after NaOH treatment for 24 hours. In contrast, the results for the NaOH treated *T. flammea flammea* do not show a clear pattern.
Due to the correlation of results of the treated *C. wallacei,* it was further tested by boiling a sample in water for 5 minutes. These results show that the wavelength increases slightly after treatment and as the angle of incidence increases, the wavelength decreases. However unlike previous results, the intensity stays almost constant.
As well as the spectrophotometer, I had the opportunity to use an SEM (Hitachi TM 3030) at St Pauls School in London. This enabled me to collect SEM images of the *C. wallacei* elytron, before and after heat and NaOH treatment and compare them to examine the effects of these environmental changes on the nanostructure. For the *T. flammea flammea*, images of the control and NaOH treated were compared (detailed analysis of results are on page 26).

3. Introduction:

Figure 1: *Iridescent properties of a soap bubble-* www.wikinut.com

3.1. Many materials possess the property of iridescence; soap bubbles (see figure 1), butterfly wings and CDs are just a few examples. Iridescence is also known as 'goniochromism', meaning that the surface of an object or material appears to change colour as the angle of viewing is altered. It only 'appears' to change colour because the illusion-like effect is created by structural coloration, not pigments. Structural coloration is caused by different wavelengths of light interacting in the nanostructure of the surface of an iridescent material. These waves of light interfere by superposing to form one resultant wave with an amplitude that is greater or smaller than the two original waves (Young 1803). Therefore, the nanostructure in the elytra of beetle wings seems to affect it's iridescent properties the most. That is, without this special structure, they would not be iridescent.

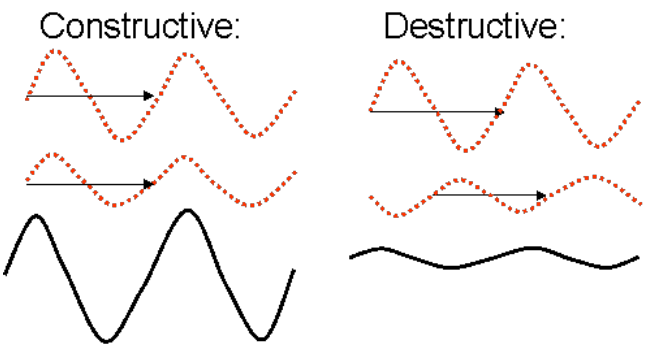

Figure 2: www.superstrate.net

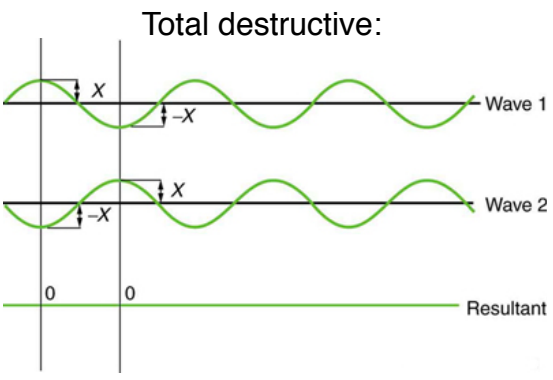

Figure 3: www.voer.edu.vn

3.2. The wave-particle duality theory suggests that light can act as a wave as well as a particle (de Broglie). Therefore, the interaction between light and iridescent surfaces can be explained by interference. Interference of two or more waves is caused by superposition. Superposition occurs when waves pass through each other; as they cross, the displacements of the two (or more) waves combine. This means that the resultant displacement equals the vector sum of the original individual displacements. There are two types of interference: constructive and destructive (see figure 2). Constructive interference involves two waves of the same frequency or wavelength travelling in the same direction, meeting and their displacements combining to give a larger displacement. In this case, the two crests add together, resulting in a larger crest; similarly, two troughs can add together to give a larger trough. This produces maxima. Two waves with a phase difference of zero or a multiple of 360 degrees, and a path difference of a whole number of wavelengths are said to be in phase.

Destructive interference is the opposite. In this case, the two waves (out of phase) are travelling in opposite directions, or they arrive out of step and are travelling in the same direction. Therefore, the displacements of the waves will subtract or produce a resultant wave, giving minima-very weak reflections. Waves with a phase difference of odd-number multiples of 180 degrees (e.g. 180 x 3 = 540 degrees), and a path difference of an odd number of half wavelengths are completely out of phase. Phase difference and path difference are different. For example, two waves can have a phase difference of 0, but their path difference can be one whole wavelength. Another type of destructive interference is total destructive interference, where two waves with equal and opposite displacements combine to cancel each other out completely (see figure 3). If the waves are only slightly in or out of phase, the magnitude of the displacement of the summed waves lies between the minimum and maximum values.

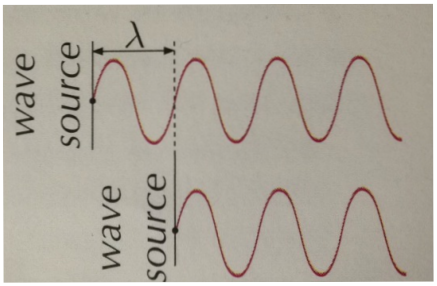

Figure 4: *Two waves that are coherent*- CGP AS level physics guide

When trying to view the maxima and minima as patterns on a screen, a coherent/monochromatic light source is usually used in order to see clear patterns. Waves are coherent when they have the same wavelength, frequency, and a fixed phase difference between them (see figure 4). Both constructive and destructive interference will occur, and which one of these is seen depends on their path difference. Visible light contains many different wavelengths, and therefore is not coherent. However, the light source that was used to collect spectra of the structural colour produced by these iridescent beetles was coherent, meaning that the waves that were reflected from the wing were maximum peak wavelengths.

3.3. All materials have a certain refractive index, a value for the ratio between the speed of light in a vacuum and the speed of light through that material. This ratio can be shown as the equation: $n=c/c_s$, where n is the refractive index of the material, c is the speed of light in a vacuum (3.00 x 10^8 m/s) and c_s is the speed of light in that material (m/s). The speed of light is smaller than c, but only by a tiny amount, so we assume that the refractive index of air is 1. The law of refraction states: "If light passes a boundary, going from a less optically dense to a more optically dense material, the light will bend towards the normal and slow down. If it goes

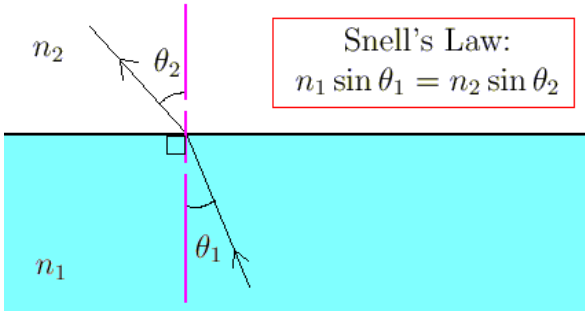

Figure 5: www.math.ubc.ca

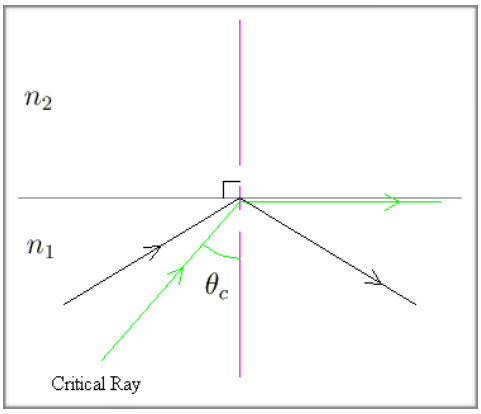

Figure 6: www.math.ubc.ca

from a more optically dense to a less optically dense material, it will bend away from the normal and speed up". This can be shown by the equations: $n_1 sin(i) = n_2 sin(r)$ or $sin(i)/sin(r) = n_2/n_1$, where n_1 is the refractive index of the first material, n_2 is the second, i is the angle of incidence of the ray in material 1, and r is the angle of refraction of the ray in material 2 (see figure 5).

The critical angle of a boundary is the angle of incidence at which the angle of refraction is 90 degrees and the angle of incidence beyond which rays totally internally reflect instead of refracting, along a more optically dense to a less optically dense medium boundary (see figure 6). The equation for the critical angle is: $sin\theta_c = n_2/n_1$. When the angle of incidence of the incident light refracting from a more optically dense layer to a less optically dense layer (e.g. for a layer-air boundary) is greater than the critical angle, absolute reflection of this light can occur. When light reflects from within the elytron, it meets the light reflected from the outer surface and interferes with it. As the angle of viewing is changed, the light will have to travel shorter/longer distances through the layers, thus meaning that different wavelengths of light will interfere and a different colour will be seen.

3.4. The most common structure responsible for this amazing display of colour, is multilayer reflectors within the surface of the material. The *Morpho rhetenor* butterfly uses this type of nanostructure, by producing a vivid blue colour that is so intense that it is said to have a visibility of up to half a mile (Vukusic *et al.* 1999). Soap bubbles also have this type of structural coloration (see figure 7). Air has a refractive index of 1, and the soap film has a refractive index of greater than 1. Some light will reflect straight off the surface of the soap film, and some will enter the soap layer and refract towards the normal, slowing down. Sometimes the angle of incidence at the next soap-air boundary will be greater than the critical angle and the light rays will reflect back into the soap film, and out of the film into the air (refracting away from the normal). At different angles, different wavelengths of light will interfere so a different colour will be produced. Film thickness also affects the type of colour created. These multilayer reflectors are present in iridescent beetles, on their own, or as well as another nanostructure such as three-dimensional photonic crystals or diffraction gratings. These different nano structures each produce a slightly different iridescent effect. The material that the layers in the nanostructure mainly consist of, is chitin. It is a long chain polymer, derived from glucose and has a very similar structure to the polysaccharide cellulose. The material does not produce iridescent properties on its own; it makes up the surfaces in the elytra that cause the interference of light.

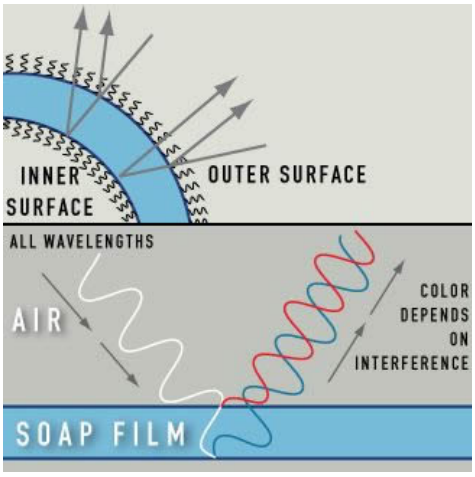

Figure 7: www.webexhibits.com

3.5. There are many natural purposes to the iridescent property of these beetles: some species use iridescence for camouflage. For instance, the green base and red stripes on the *C. fulgidissima*

fulgidissima and *T. flammea* match surrounding leaves and flowers. This enables them to avoid being eaten by predators (e.g. birds).
Interspecific and intraspecific communication is another example. Individuals can recognise and communicate with members of their own species or between species. Structural colour causes iridescence. It is brighter and more intense than pigmented colour, so it can be seen from several meters away even in low light areas such as forests where light penetration can be as low as 2 percent.
Other advantages include mate choice, orientation and schooling, deterring predators by exhibiting warning colours, thermoregulation, friction reduction, water repelling, strengthening, and vision enhancement.

4. Literature review:

4.1. Pigment or structure?
Many scientists have concluded that iridescence is a unique property of structural colour, and is not caused by pigments. Glover *et al.* (2010) explained why:
"Chemical and structural colours have several different properties. They differ first in the intensity of colour that they produce". Pigments produced by chemicals are less intense than structural colours because they absorb most wavelengths of light and cannot selectively absorb a few wavelengths. Therefore a broad range of wavelengths is reflected from pigments. However, structural colours appear very intense as they only absorb and reflect a few wavelengths of light. Structural colour also lasts longer than pigmented colour. Although the colour reflected from a beetle can change slightly over time, its iridescent properties will last even after its death. This is because chitin is a straight chain molecule that can hydrogen bond to other chains to create a strong rigid lattice that is very difficult to break. This minimises any damage to the layers in the nanostructure, which allows a long-lasting iridescent effect.
Chemical pigments found in materials are spread over the surface of a material, and produce colour which is perceived to be the same from all angles. Different pigments on the petals of plants (for example in veins) show this pattern.
In contrast, structural colour allows a shift in colour to occur as the angle of observation is altered. This is a characteristic property of iridescence. The wavelengths reflected from iridescent surfaces can belong to any part of the electromagnetic spectrum but is intrinsic to any given structure. However, the ones that we see are only those that occur within the visible range.

4.2. As described earlier, the type of iridescence a material has can be classified into three classes: thin film multilayer reflectors, three-dimensional photonic crystals and diffraction gratings. These different nano structures cause the incident light rays to interfere in different ways, and therefore produce different intensities and wavelengths of light that give different iridescent properties. An article by Seago *et al.* (2009) titled "Gold bugs and beyond: a review of iridescence and structural colour mechanisms in beetles (*Coleoptera*)" explains how these structures differ.
4.2.1. Multilayer reflectors (see figure 8) also known as 'thin-film reflectors' or 'one-dimensional photonics crystals', are the most common nanostructure in elytra of iridescent beetles. Certain species have evolved to create this impressive nanostructure by themselves: "During the formation of insect integument, thin parallel layers of chitin (sometimes interspersed with other materials) that differ in refractive index are secreted by the epidermis and later harden during sclerotisation" (Seago *et al.* 2009). With a multilayer reflector, one or several colours are produced by constructive interference when the spacing between the layers becomes a quarter of the

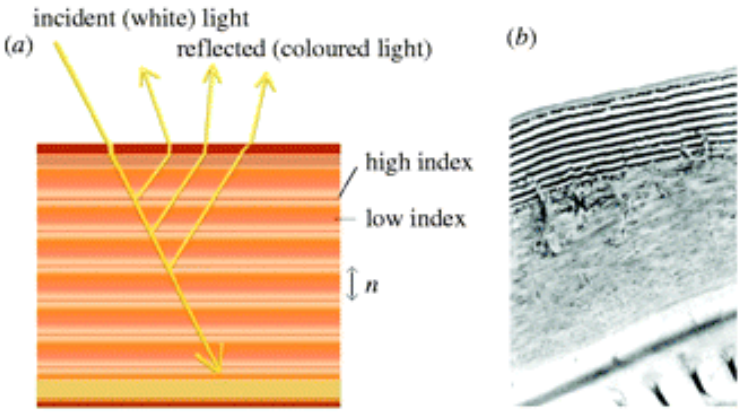

Figure 8: *(a) Simple diagram of multilayer cuticular reflector, (b) TEM cross section of cuticular reflector of Cicindela scutellaris*- Seago *et al.* 2009

wavelength of incident light. Some of the incident white light is reflected straight off of the surface of the first layer, but some refracts through the layers. Shorter wavelengths refract more than longer wavelengths, resulting in only selective wavelengths being reflected. When the angle of incidence of the incident light refracting from a more optical dense layer to a less optical dense layer (e.g. for a layer-air boundary) is greater than the critical angle, absolute reflection of this light can occur. Some wavelengths of light reflected from the deeper layers will produce colours by interfering with the waves that reflect from the outer surface but some will not, due to being reflected from layers with a different refractive index and some travelling more than others. They will interfere constructively or destructively depending on their path difference. Constructively interfered wavelengths produce the vivid colours that we see on iridescent beetles.

The path difference also determines whether the waves are in phase or out of phase and so whether constructive or destructive interference occurs. Waves that have a path difference of a whole number of wavelengths are in phase and will constructively interfere, producing maxima of very intense colours. Those that have a path difference of a half wavelength, one and a half wavelengths, two and a half wavelengths etc., are out of phase, and will destructively interfere, producing minima and giving very weak colour or no colour at all. This path difference is due to and dependent on the thickness and refractive index of the layer or layers it travels through, the light's wavelength and angle of incidence at which the light ray reaches the boundary.

Therefore, the type of structural colour produced from a multilayer structure depends on the refractive indices of the chitin layers, their thickness and the difference in refractive index between the layers and surrounding air. This is because "Layers with a greater optical thickness reflect longer wavelengths than optically thinner layers and the peak wavelength$_{max}$ is equal to $2(n_a d_a C n_b d_b)$, where n is the refractive index; d is the actual layer thickness; a and b are the alternating layers in the reflector" (Land 1972, cited by Seago *et al.* 2009). Elytra of each species of beetle consist of layers with different optical thicknesses. This means that the structural colour reflected will be different for the four types of beetles that will be tested in this investigation.

As the angle of incidence of white light changes, the path differences will change and therefore different wavelengths will constructively interfere. More specifically, "as the angle of observation increases, the reflected colour will undergo a 'blue shift' to a shorter wavelength (see Vigneron *et al*. (2006) and Kinoshita *et al*. (2008) for photographic illustration)…because reflected light rays are travelling a shorter distance throughout each layer, which means that constructive interference occurs for shorter wavelengths" (Seago *et al.* 2009) and the longer wavelengths interfere destructively, so the shorter wavelengths are the ones reflected and seen. This perhaps implies that the wavelengths reflected from the deeper layers will travel diagonally across upper layers but because the wing is curved they will travel a shorter distance to reach the surrounding air. The layers may also vary in thickness from the centre to the edge of the elytron. For example, the order *Coleoptera* has many parallel layers present, which shift in layer thickness which produces an effective cuticular reflector ('Nature's Nanostructures'- Amanda S. Barnard *et al.* 2008). This

supports the original results that were obtained by all of the beetles we tested, where the peak wavelength generally shifted to the left on the graph. We suspected that the beetles only possessed this structure and our working hypothesis was that the structural colour produced by the *C. wallacei* was due to a multilayer reflector. However, now we suspect that the *C. wallacei'*s nanostructure is not as simple as the multilayer structure, due to the complex structures of the elytra seen on the SEM and results obtained from using a sodium lamp.

4.2.2. Three-dimensional photonic crystals (see figure 9) are rare crystalline structures producing a

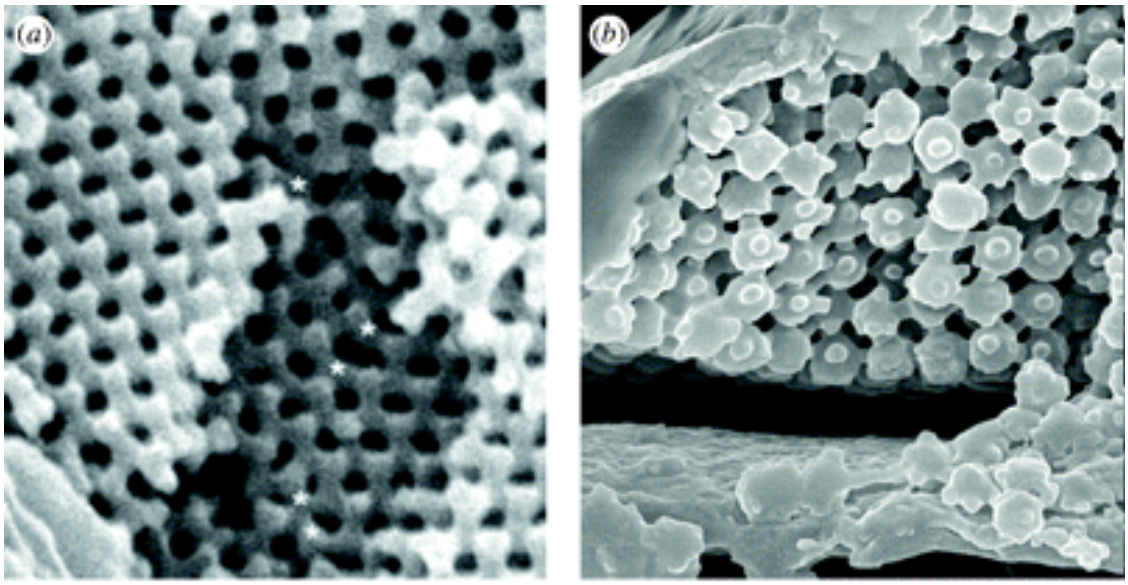

Figure 9: (*a*) *Pachyrrhynchus congestus pavonius*- SEM of crystal structure from scale interior (from Welch & Vigneron 2007), (*b*) SEM of the interior structure of *Prosopocerus lactator*- Seago *et al.* 2009

"scintillating, gem-like reflectance". The specific nanostructure may vary between species of insects: "The photonic crystals found in the scales of pachyrrhynchine weevils (*Pachyrrhynchus* and *Metapocrytus*) have a close-packed hexagonal arrangement analogous to (mineral) opal, while the photonic crystal of *Lamprocyphus* has a diamond-based lattice facing different directions (i.e. a face-centred cubic system rather than a hexagonal one)" (Seago *et al.* 2009). The scales of the *Lamprocyphus* are said to be divided into pixels that are one micrometer wide, each being a single crystal and reflecting light in a unique direction.

With the photonic crystals of the *Lamprocyphus*, structural colour is produced by a highly ordered lattice of nanoscale spheres in the interior of flattened scales. These structures are said to be 'iridescent-reducing'; they reflect vivid, saturated interference colours but reduce the angle dependancy of the chromatic effect. This may be a result of the reflectors being divergent to each other and the exoskeleton of the organism.

As well as these types of lattices, there is also the gyroid-like lattice, commonly found in iridescent butterflies, for example the *Callophrys rubi* (Seago *et al.* 2009). The cuticular three-dimensional structure is created by gyroid membranes that are found in the smooth endoplasmic reticulum in the cells of the scales. When the cells die, the cubic membranes dry and harden to leave behind a cuticular structure (K Michielsen *et al.* 2008, cited by Seago *et al.* 2009). Some species of Longhorn beetles (e.g. family *Cerambycidae*) also possess this nanostructure.

Research into this three dimensional structure has only just begun; in fact, it was only discovered to be present very recently. The mechanism of this structure and incident light has not yet been explained. It is possible that there are many multilayer reflectors within the three-dimensional structure, that is more selective in reflecting wavelengths of light, due to its complexity. It may be

that the *C. wallacei* possesses this structure, due to the complex SEM images of it's cross-layering and slightly reduced iridescence, but this has not yet been investigated due to the rarity of the structure: "three-dimensional photonic crystals have never been observed in any beetle group without scales, nor have they been observed elsewhere in the integument. This pattern is remarkably conservative throughout insects: the 2-D and 3-D photonic crystals of moths, butterflies and bees are all restricted to the lumen of scales and similarly modified hollow setae." (Barnard *et al.* 2008, cited by Seago *et al.* 2009).

4.2.3. Two dimensional diffraction gratings consist of parallel ridges or slits that disperse light into its constituent wavelengths (see figure 10 *(a)*). The direction of the reflected beams depends on the spacing of the gratings. When white light is passed through a diffraction grating, the reflected light will have rainbow-like properties because it will diffract into full spectra of all possible wavelengths. Beetles that use this type of structure produce iridescence by dispersing light via

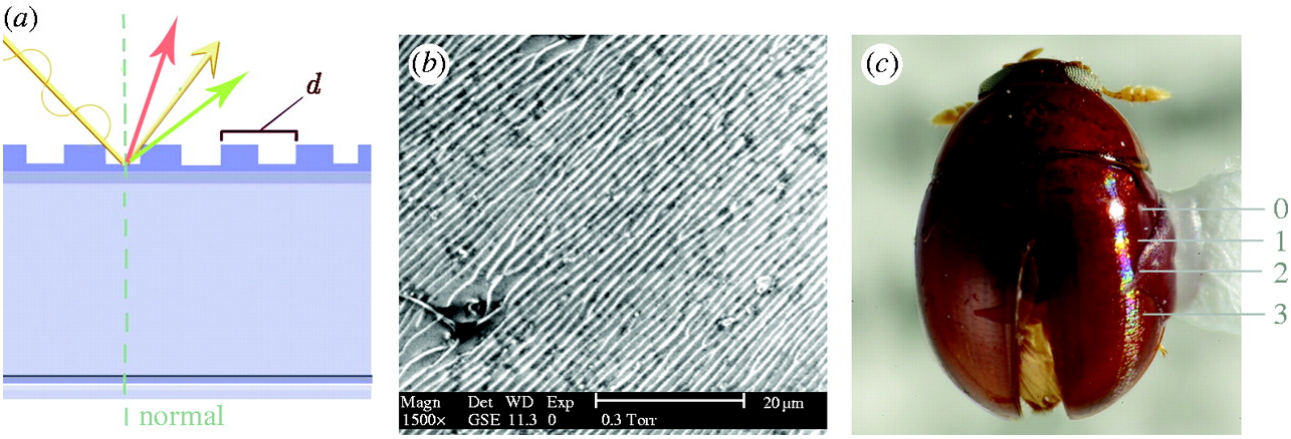

Figure 10: (*a*) Schematic of cuticular grating, (*b*) SEM of diffraction grating, Sphaeridiinae gen. sp. (Hydrophilidae), and (*c*) Sphaeridiinae gen. sp., habitus view with zero, first, second and third spectral orders labelled- Seago *et al.* 2009

natural reflection only, as opposed to transmission in man-made diffraction gratings.

"Iridescence arising from diffraction gratings always takes the form of one or more ordered spectra —that is, colours are ordered in the same sequence as the colours in the spectrum of visible light, red–orange–yellow–green–blue–violet" (Seago *et al.* 2009), unlike multilayer structures that are unordered. They follow a sequence of spectral orders, from zero-order, first-order (saturated red/ yellow/blue) to high-order spectra of secondary colours.

4.3. Iridescent colours can change due to environmental changes or during development. For example, the humidity, temperature of the surroundings, and certain chemicals can affect the colour patterns produced.

As some beetles develop, the reflected wavelengths will change because the optical thickness of the multilayers will change. This occurs in some donaciine chrysomelids, in which adults undergo a non reversible shift from metallic blue to green over the course of several months (M. Barclay 2008, cited by Seago *et al.* 2009). This may be due to the chitin layers hardening during sclerotisation. During this period, dehydration of the layers may reduce the number or types of wavelengths reflected (Schultz & Rankin 1985, cited by *Seago et al.* 2009). The pores in the elytra, perhaps used as spiracles, allow gases and liquids to pass in between the layers which changes the refractive index of air in between the layers. This will permanently change the colour of the beetle, as different wavelengths will be reflected. However, permanent colour change due to environmental

change can only be achieved when the multilayer is put under extreme stress (tension, heat, etc.), which will alter the refractive indices of the layers of chitin. For example, the colour of the buprestid (*Chrysochroa*) elytra can be changed by heating the sample to 200°C or by soaking it in bromoform for one month (Adachi 2007). Another example is a staphylinid specimen, that was affected by long term UV exposure (S. Chatzimanolis 2008). The specimen was partially left in sunlight for over 20 years which caused the exposed side of the beetle to lose its metallic colours. 'Hygrochromic colours' are structural colours that can be reversibly changed (Mason 1929; Hinton 1973*a*,*b*; Rassart *et al*. 2008). Beebe (1947) and Hinton & Jarman (1972) described the colour change in the species *Dynastes hercules;* the 'resting state' elytral coloration of greenish-grey changes to black when hydrated but this change only occurred in males (Rassart *et al*. 2008) and can also be induced by applying strong mechanical stress (cited by Seago *et. al* 2009). Unlike the multilayer structure, the hygrochromic structure is an ordered lattice with porous regions. The mechanism to how these changes occur was also explained: "as moisture infiltrates the spaces, the difference in refractive index between chitin and lacunae—and thus the amount of scattering/ reflection—is decreased dramatically, more light is absorbed, and the elytron appears black in colour" (Hinton & Jarman 1972; Hinton 1973*a*; Rassart *et al*. 2008).
In addition, a thorough study of the colour change mechanism in *C. egregia* concluded that the original gold colour of this species is produced in the exocuticle by a broadband reflector (multilayer structure) that consists of high-index porous chitin layers. A change of colour from gold to red is caused by dehydration, as opposed to the hydration of *D. hercules* (Vigneron *et al*. 2007, cited by Seago *et al.* 2009). Dehydration occurs as the moisture in between the layers escapes from the pores in the layers, which collapses the multilayer reflector into a 'translucent stack'. Therefore, the change in refractive index between adjacent layers becomes low enough to allow most incident light to refract and be absorbed, apart from the red wavelengths.

5. Experiment:

5.1. Hypotheses:

I have a number of questions that I would like to answer. My questions include:
- How will the wavelength change as the angle of incidence is increased for the *C. wallacei* and *T. flammea flammea*?
- If heating, dehydrating or boiling affects the *C. wallacei*, how will it affect the wavelength and intensity of light reflected?
- If dehydrating affects the *T. flammea flammea*, how will it affect the wavelength and intensity of light reflected?
- If the *C. wallacei* is affected by heat, is the change reversible?

These are my predictions:
- For the *C. Wallacei* beetle, as the angle of incidence increases the peak wavelength will move to the left/ decrease. I predict this because Vigneron *et al*. (2006) and Kinoshita *et al*. (2008) stated that the shorter wavelengths are reflected at greater angles as light has to travel a shorter distance through the layers of the nanostructure.
- For the *T. flammea flammea* beetle, the pattern will be the same but the peak wavelengths will in general be higher and shift will be greater. This is because there is a red stripe on the centre of the elytron, where the light is shone. The wavelength of red light is significantly higher than the wavelength of blue or green light, and as the angle of incidence increases the light will diagonally reflect through the layers and shorter wavelengths will be reflected.

- The peak wavelength for the heated *C. wallacei* will be lower than the peak wavelength for the control *C. wallacei*. I suspect this because the heat will cause the moisture in the layers or between the layers to evaporate so the optical thickness of the chitin layers will decrease. Land (1972) concluded that layers with a greater optical thickness reflect longer wavelengths, therefore the heated chitin layers will reflect shorter wavelengths and absorb longer wavelengths.
- Dehydrating the *C. wallacei* and *T. flammea flammea* will cause their peak wavelengths to decrease, but they will still decrease as the angle of incidence is increased. This is because dehydration will cause the same effect as heating; moisture in the nanostructure will evaporate through the pores and the optical thickness of the chitin layers will decrease so they will reflect shorter wavelengths.
- Boiling the *C. wallacei* will cause the peak wavelength to increase, but the wavelength will still decrease as the angle of incidence is increased. I predict this because boiling the elytron may cause water to enter the nanostructure via the pores and Hinton & Jarman 1972 stated that if moisture enters in between the layers of chitin, the difference in refractive index between the layers and air will decrease. Also, the optical thickness of the layers may increase. This means that higher wavelengths will be reflected.

5.2. Equipment:

- SpectraSuite software
- Ocean Optics 1000μm diameter Optical Fibres
- Goniometer
- *Chrysochroa wallacei* and *Torynorrhina flammea flammea* beetle elytra
- Red and green card
- Scalpel
- Tweezers
- Needle/pin
- Infrared Thermometer Gun
- Microscope slides
- Ocean Optics USB-650 Red Tide Spectrophotometer
- Ocean Optics Halogen Light Source HL-2000 (%vdc/ 1435a output to bulb. Focussed. Bulb colour temperature: 2.960k with power: 7w)
- Oven
- NaOH and Anhydrous Calcium Chloride
- Test tube
- Heat resistant gloves
- Sample tubes

5.3. Method:

1. The software SpectraSuite was downloaded onto the laptop and an optical fibre connected the laptop to the spectrophotometer, which was connected to the clamped receiver. Another optical fibre was used to connect the halogen light source to the other clamp so that the diameter of light coming from the light source was as small as possible. The clamps were set up so that they were at the same vertical level and were perfectly aligned. This was done by moving the receiver 180 degrees away from the clamped light source and making sure that the angle on the goniometer read ‘180 degrees’. A pen was then used to line the clamps up and make sure that

the clamps were parallel to each other and the rotating frame. I also made sure that the rotating frame was exactly halfway between the two clamps.

2. Next, the light source and spectrophotometer were turned on and I made sure that the light was covering the receiver fully and a spectra was being produced, of the wavelength and intensity of light received on SpectraSuite. The spectra of white light was removed so that it did not affect the results of the reflected light.

Red and green card

3. A piece of red card was clamped in between two slides and this was put in the rotating frame. The light was shone on the card and I made sure that the area that was covered by the light was not covered by glass.
4. The blind was pulled down and the light was turned off. The light source was also switched off and any background light was also eliminated on SpectraSuite by removing the dark light spectra because this would also skew the results. The integration time was set to an appropriate number, by selecting the integration time that produced the largest intensity on the spectra. This integration time was kept constant throughout the experiment.
5. The light source was then switched back on and the first angle of incidence of 15 degrees was set on the goniometer by moving the receiver. A spectra was collected for each angle of incidence on SpectraSuite, until 35 degrees at 5 degree intervals. These graphs were collected and overlapped. This process was repeated for the green card.

Heat control of *C. wallacei*

6. Then, an elytron of the heat controlled C. wallacei (before heating) was cut off using a scalpel and the base of the elytron (the widest part that is connected to the thorax) was carefully clamped between two slides using some tweezers to flatten the beetle as much as possible. The two slides were held together using some pegs and clamped into the rotating frame on the goniometer. The elytron was quite curved, therefore to minimise anomalous results a pin was clamped holding the tip of the elytron so that it was straighter. The area of the elytron that the light was shone could not be covered by glass or the pin because this would affect the wavelengths reflected from it.
7. The receiver was pulled towards the light source so that the difference between them was 30 degrees and their normal was perpendicular to the elytron, therefore meaning that the angle of incidence was 15 degrees. I altered the position of the clamped elytron so that the light was shining directly at the centre of it, and it was in line with the axis of rotation so that when the angle of incidence was altered the spot of light would not move. Again, I made sure that the elytron was perpendicular to the normal of the receiver and light source.
8. Background light was removed in the same way as with the card. The integration time was also set to the right setting. Keeping the blind down and the room light switched off, the light source was switched back on again. The spectra for 15 degrees was saved and the receiver was moved so that the angle on the goniometer read ’36 degrees’ and the angle of incidence was 18 degrees. The elytron on the rotating frame was rotated so that it was perpendicular to the normal again. The spectra was saved and this process was repeated until the angle of incidence was 36 degrees, at 3 degree intervals.
9. After all the graphs were collected, a graph overlay was created on SpectraSuite by overlapping the graphs for all the angles.
10. Several SEM images were taken of the underside, top surface and side of the controlled elytron.

Heat treated *C. wallacei*

11. The same elytron was then heated (still in the clamp) in a preheated oven for 20 minutes. It was taken out carefully and put in the rotating frame. The angle of incidence was reduced back to 15 degrees and the temperature of elytron was recorded every 30 seconds using an infrared gun. Graphs for at least 5 different temperatures were produced whilst keeping the angle constant. Gloves were worn when handling the heated elytron for safety.
12. The previous step was repeated for angles of 18, 21, 24, 27 and 30 degrees, each time heating a new elytron of the same species and size. The spectra of wavelength against intensity for the decreasing temperatures was put together as a graph overlay for each angle. These made up the first set of results.
13. Then, another elytron was heated in the same way for the same amount of time. 0 hours after heating, graphs were produced at angles 15 to 36 degrees at 3 degree intervals. Therefore the elytron cooled while the angle was increased. The graphs were overlapped and this was repeated for 1 hour, 2 hours and 3 hours after heating.
14. The same elytron was heated for the second time in the oven, for 20 minutes. The angle was increased again at the same intervals and the graphs were produced and put together.
15. Images of the underside, ripped edge and iridescent surface were taken on the SEM.

NaOH control and treated *C. wallacei*

16. Another elytron was taken as a control and its spectra were collected from 15 degrees to 36 degrees at 3 degree intervals. The same elytron was then put in a solution of NaOH and water in a sample tube and later dehydrated with Anhydrous Calcium Chloride. The sample was left for a week, and taken out carefully. A collection of graphs was produced from 18 degrees to 30 degrees at 2 degree intervals.
17. Images of the NaOH treated and control were taken on the SEM.

NaOH control and treated *T. flammea flammea*

18. The previous step was then repeated for the *T. flammea flammea*. The reflected light of the controlled elytra was measured from 15 degrees to 65 degrees at 5 degree intervals. The elytron was soaked in the same chemicals for the same amount of time and was measured from 15 degrees to 35 degrees at 2.5 degree intervals.
19. Again, images of the NaOH treated and control were taken on the SEM at several areas of the elytron.

Boiled *C. wallacei*

20. An elytron of a C. wallacei beetle was put in a boiling tube with water and boiled with a bunsen burner for around 5 minutes until its colour changed. The infrared thermometer gun was used to make sure that its temperature had increased significantly. The tube was held with tongs and googles were worn for protection. The tube was passed through the flame with regular breaks so that carbon would not accumulate and the water would not evaporate.
21. The wing case was then transported from the lab to the goniometer in a sample tube. The elytron was taken out with tweezers, carefully placed in between the slides and clamped in the frame. A spectra was collected every 3 degrees, from 15 degrees to 45 degrees. The graphs were then overlaid on SpectraSuite.

St Pauls School in London prepared the elytra for viewing with an SEM. The samples of elytra were ripped and placed on a disk. Each disc was used to balance several samples of the same elytron and the discs were numbered so that when they were viewed on the computer, it would be easy to find

out whether it was a control or treated. It was lightly sprayed with gold so that there was a layer of electrically conducting material around the sample and the sample itself would not become charged by the electron beam. Four of the discs were placed on a plate and this was inserted into the SEM chamber. The SEM was turned on, the image of the chamber was viewed on the computer by using the software. The knobs on the machine were used to direct the camera to the area that I wanted to look at. Then, the focus and magnification was adjusted so that the desired image was as clear as possible.

5.4. Results:

Key:
1a) Red card overlay- 15 degrees to 35 degrees at 5 degree intervals.
1b) Green card overlay-15 degrees to 35 degrees at 5 degree intervals.
Heated *C. wallacei*:
2a) 15 degrees every 30 seconds
2b) 18 degrees every 30 seconds
2c) 21 degrees every 30 seconds
2d) 24 degrees every 30 seconds
2e) 27 degrees every 30 seconds
2f) 30 degrees every 30 seconds
2g) Heat control
3a) 0 hours after
3b) 1 hour after
3c) 2 hours after
3d) 3 hours after
3e) After second heating
NaOH treated *C. wallacei*:
4a) NaOH control
4b) After NaOH
NaOH treated *T. flammea flammea*:
5a) NaOH control
5b) NaOH treated
Boiled *C. wallacei*:
6a) After 5 minutes of boiling
SEM images:
7a) *C. wallacei* heat control top surface from first visit, magnification x600
7b) *C. wallacei* heat control ripped edge from second visit, magnification x300
7c) *C. wallacei* after heat top surface from first visit, magnification x4000
7d) *C. wallacei* after heat ripped edge from second visit, magnification x200
7e) *C. wallacei* NaOH control, magnification x800
7f) *C. wallacei* after NaOH ripped edge, magnification x1500
7g) *C. wallacei* after NaOH top surface with a crack, magnification x2500
7h) *T. flammea flammea* NaOH control ripped edge, magnification x100
7i) *T. flammea flammea* after NaOH ripped edge, magnification x300

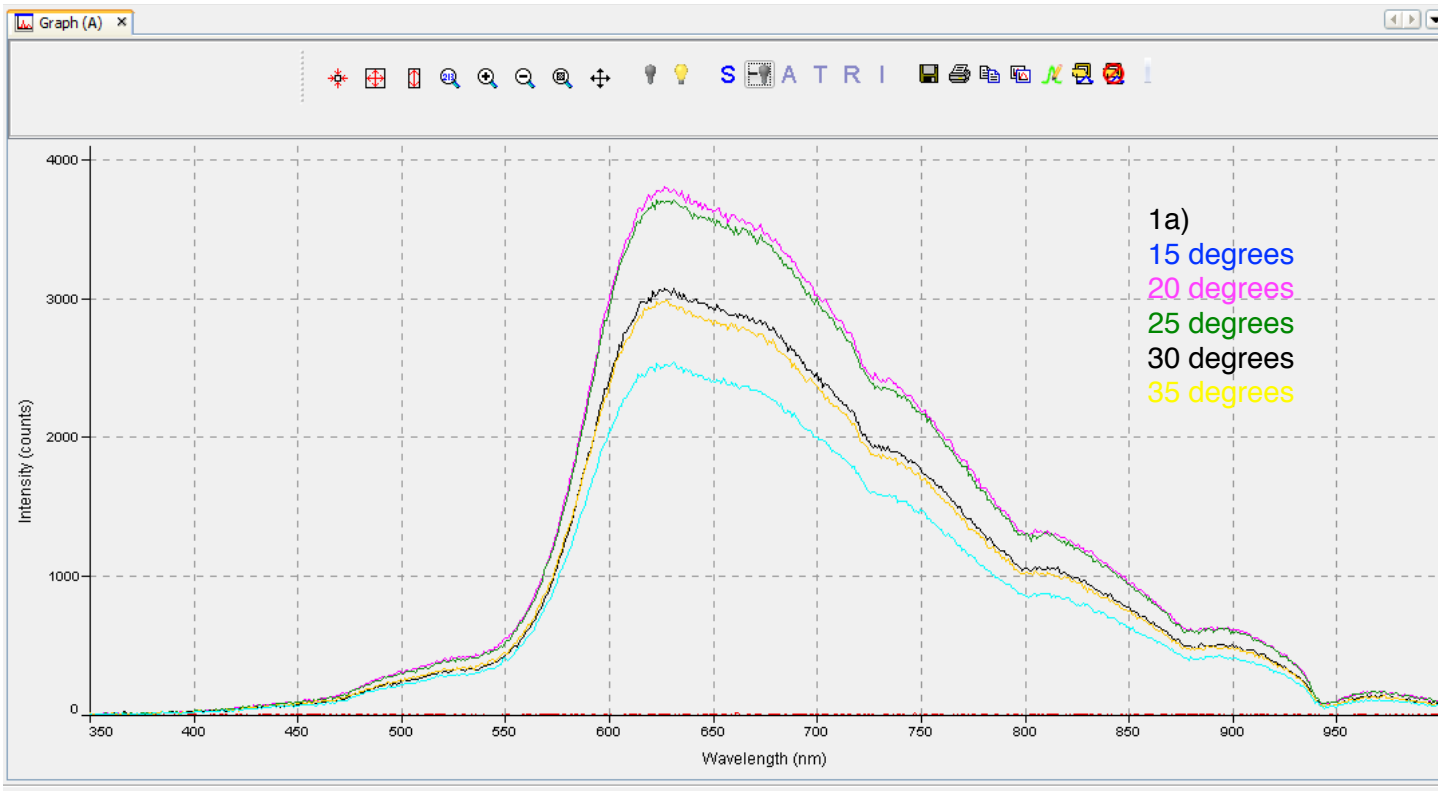
Graph (A)
1a)
15 degrees
20 degrees
25 degrees
30 degrees
35 degrees
Intensity (counts)
Wavelength (nm)
0
1000
2000
3000
4000
350
400
450
500
550
600
650
700
750
800
850
900
950

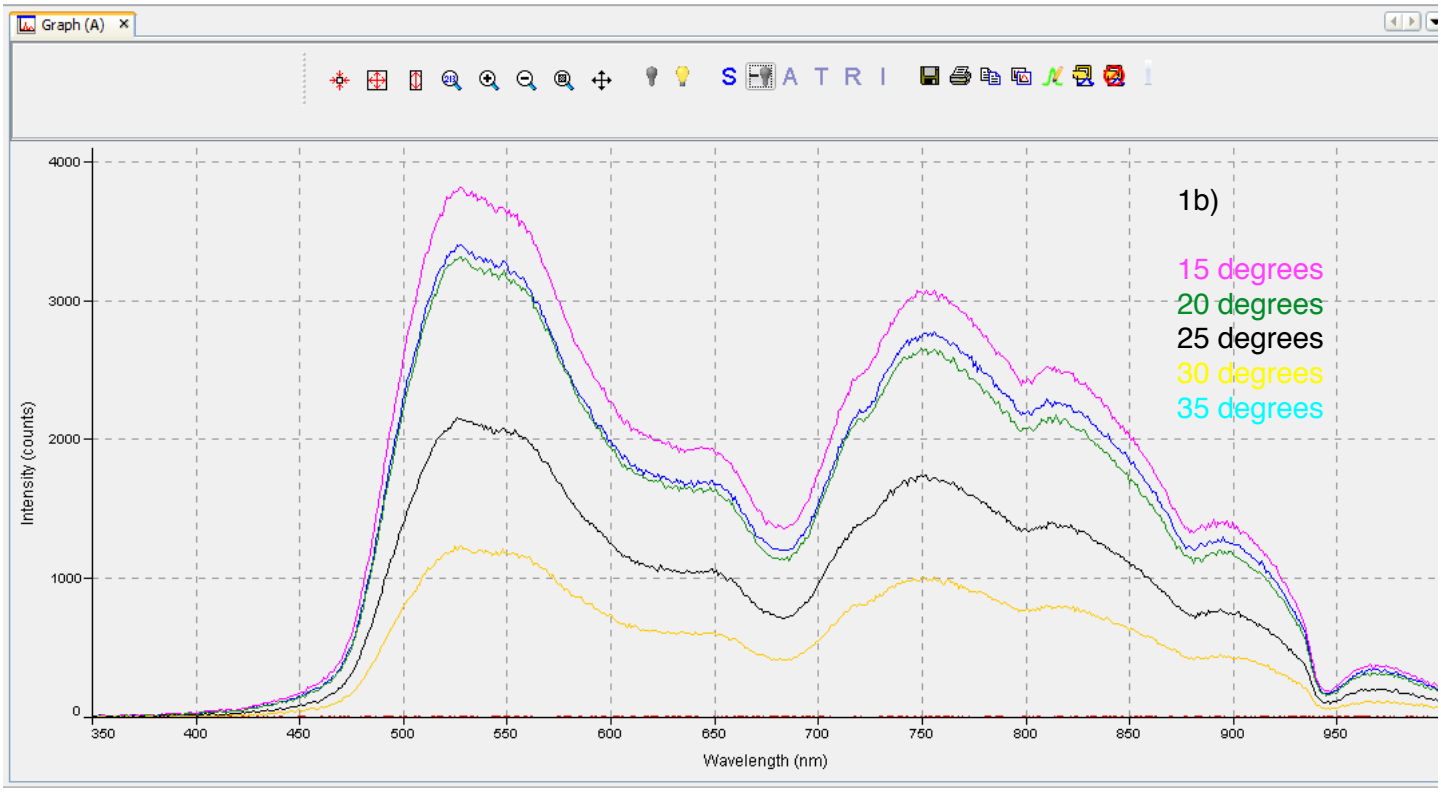
Graph (A)
1b)
15 degrees
20 degrees
25 degrees
30 degrees
35 degrees
Intensity (counts)
Wavelength (nm)
0
1000
2000
3000
4000
350
400
450
500
550
600
650
700
750
800
850
900
950

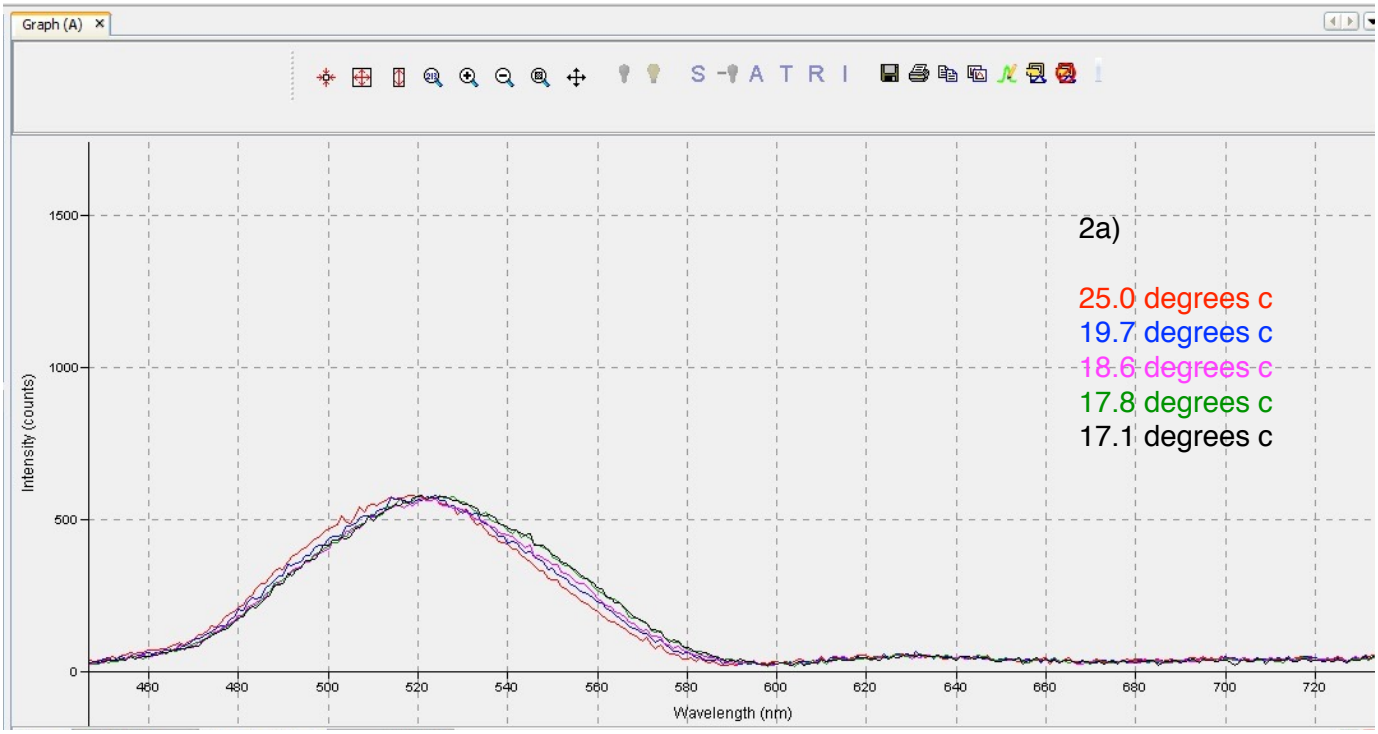
Graph (A)
S-A T R I
2a)
25.0 degrees c
19.7 degrees c
18.6 degrees c
17.8 degrees c
17.1 degrees c
Intensity (counts)
Wavelength (nm)
0
500
1000
1500
460
480
500
520
540
560
580
600
620
640
660
680
700
720

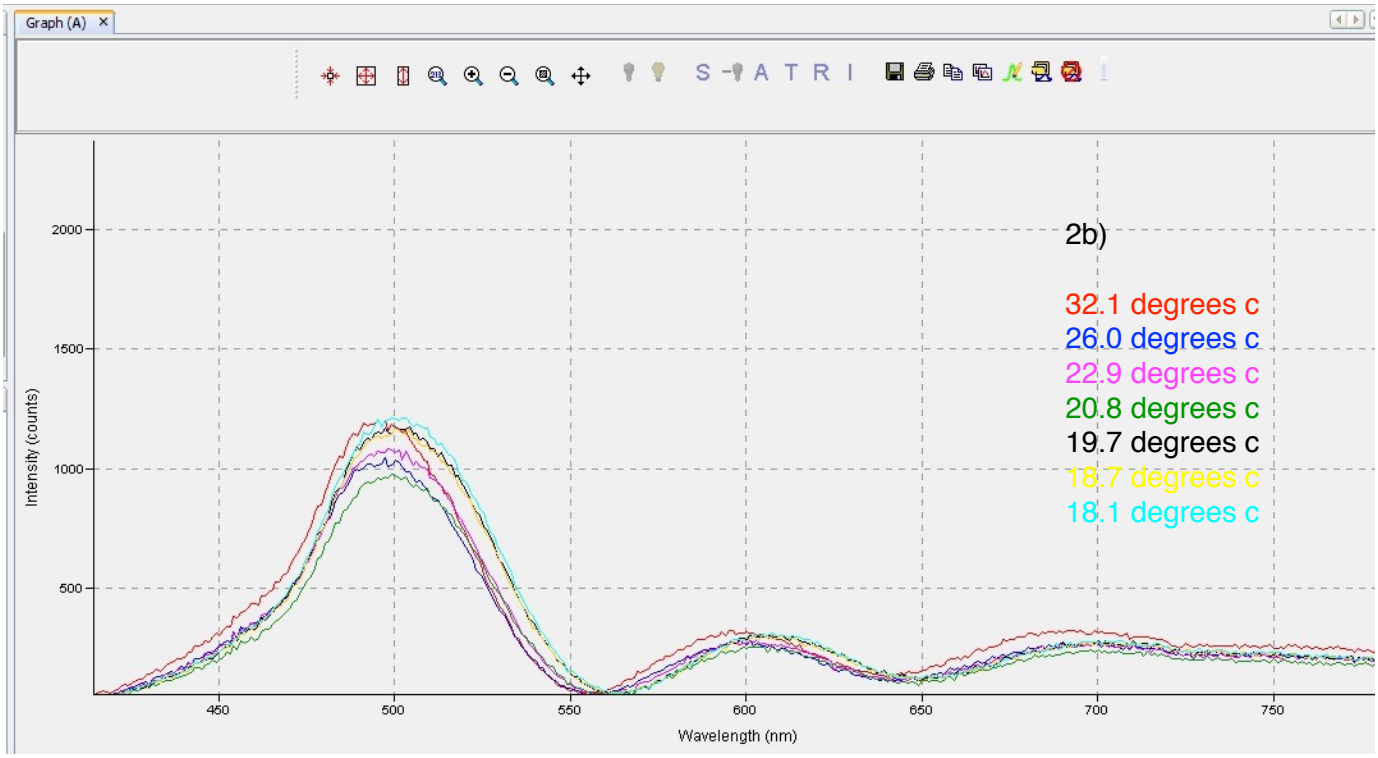
Graph (A)
S-A T R I
2b)
32.1 degrees c
26.0 degrees c
22.9 degrees c
20.8 degrees c
19.7 degrees c
18.7 degrees c
18.1 degrees c
Intensity (counts)
Wavelength (nm)
500
1000
1500
2000
450
500
550
600
650
700
750

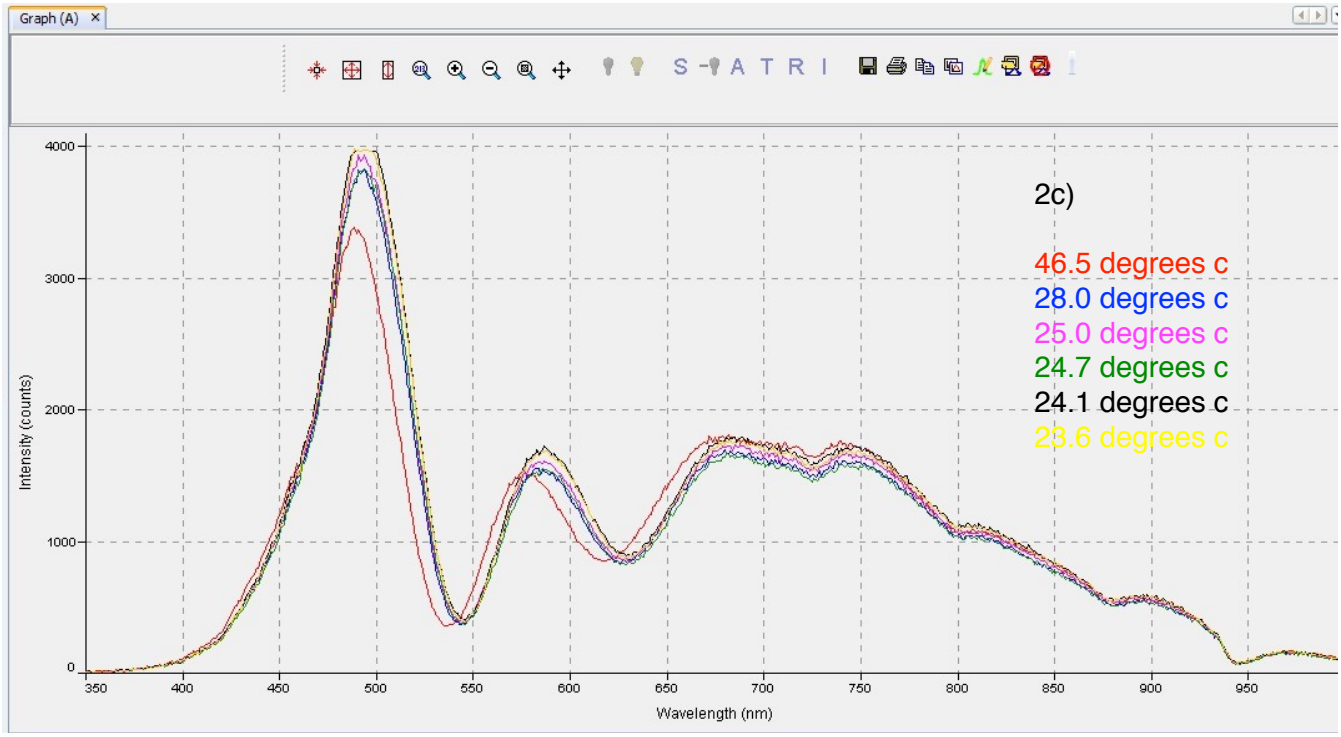
Graph (A)
S-A T R I
2c)
46.5 degrees c
28.0 degrees c
25.0 degrees c
24.7 degrees c
24.1 degrees c
23.6 degrees c
Intensity (counts)
Wavelength (nm)
0
1000
2000
3000
4000
350
400
450
500
550
600
650
700
750
800
850
900
950

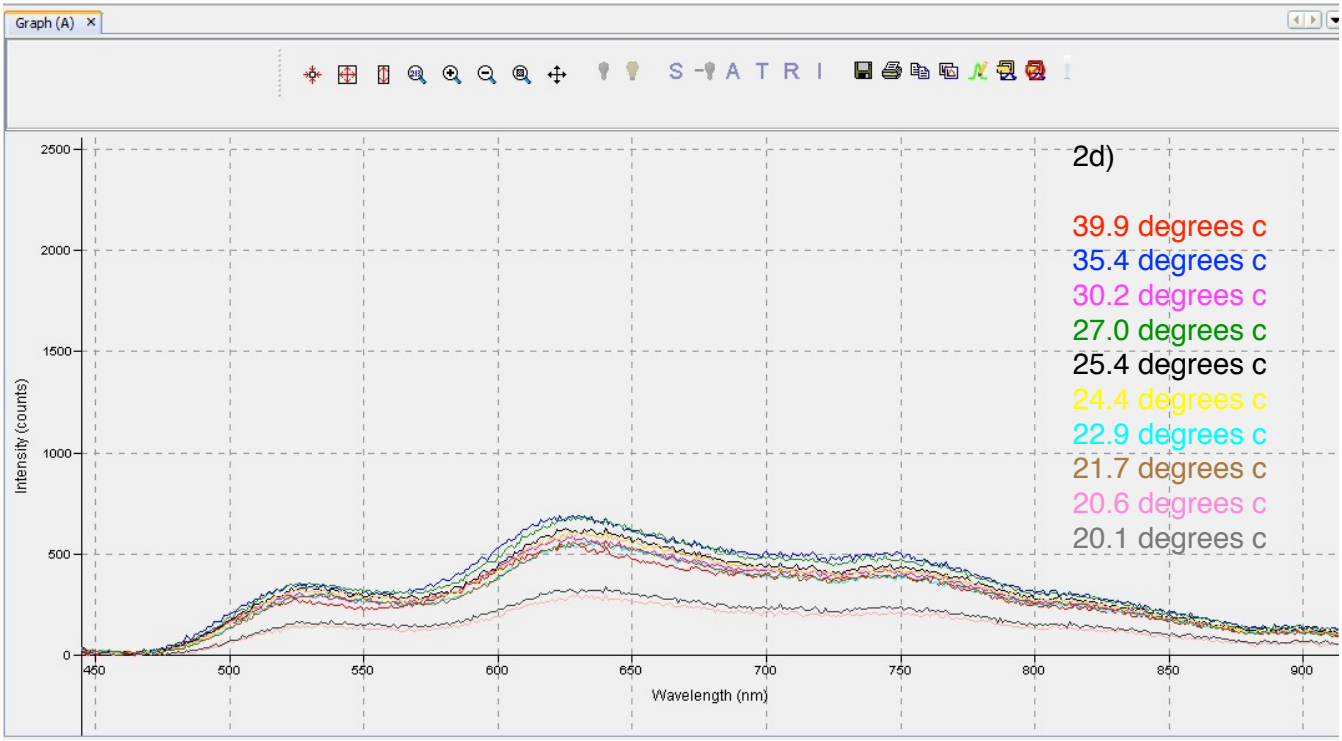
Graph (A)
S-A T R I
2d)
39.9 degrees c
35.4 degrees c
30.2 degrees c
27.0 degrees c
25.4 degrees c
24.4 degrees c
22.9 degrees c
21.7 degrees c
20.6 degrees c
20.1 degrees c
Intensity (counts)
Wavelength (nm)
0
500
1000
1500
2000
2500
450
500
550
600
650
700
750
800
850
900

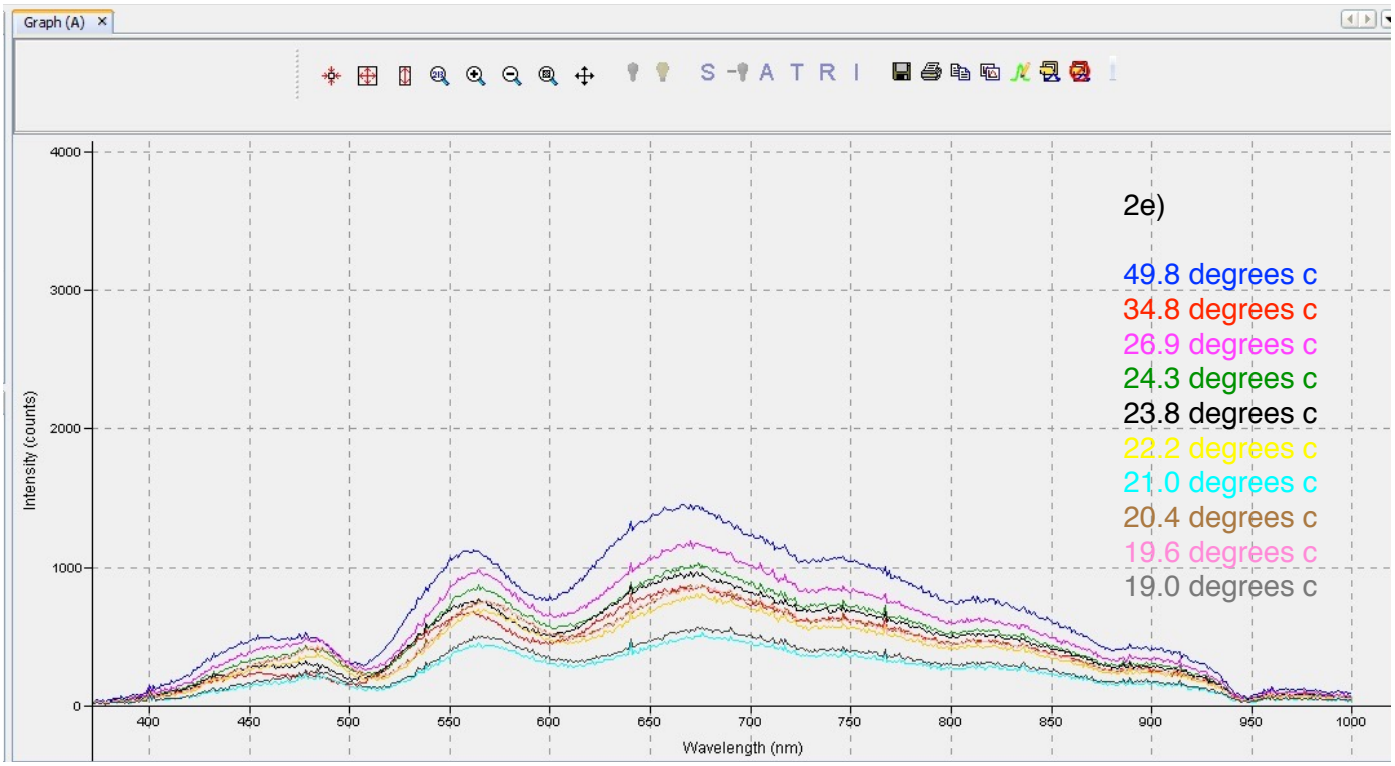
Graph (A)
S-A T R I
2e)
49.8 degrees c
34.8 degrees c
26.9 degrees c
24.3 degrees c
23.8 degrees c
22.2 degrees c
21.0 degrees c
20.4 degrees c
19.6 degrees c
19.0 degrees c
Intensity (counts)
Wavelength (nm)

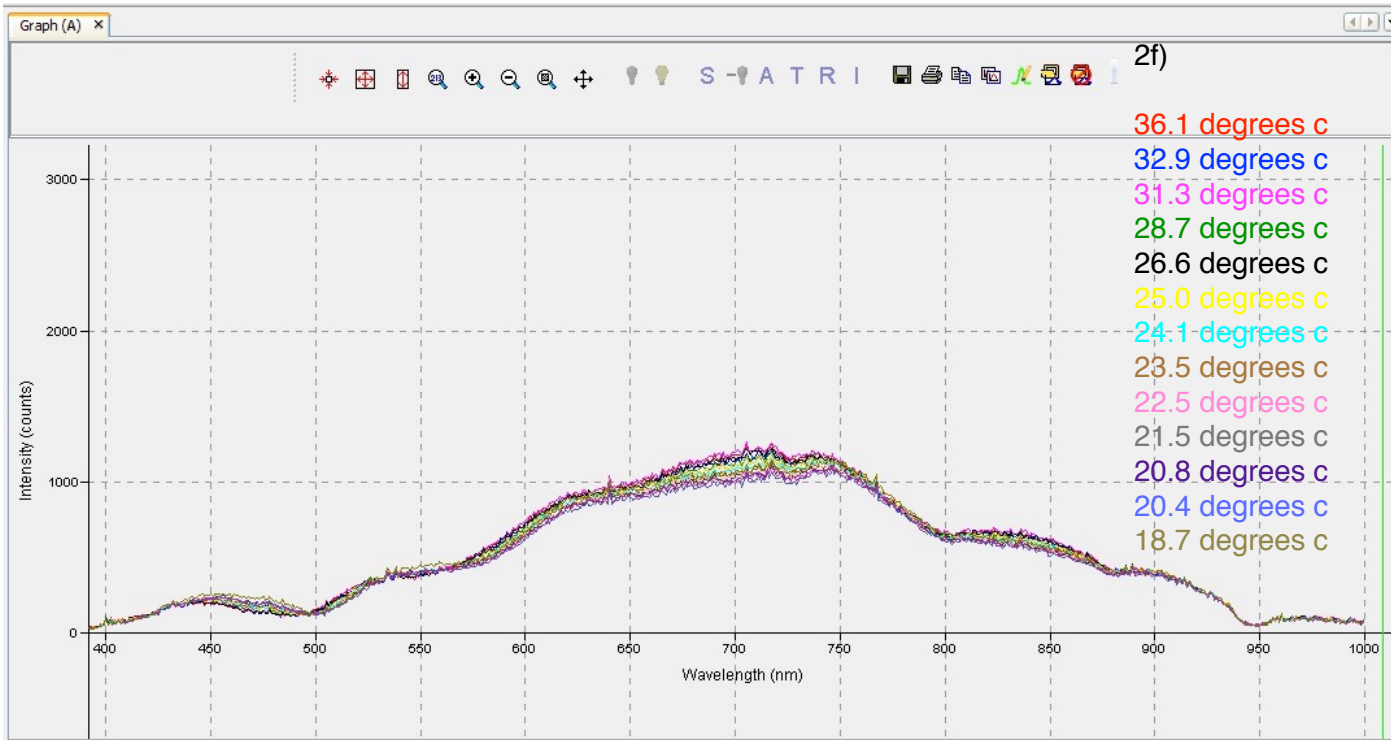
Graph (A)
S-A T R I
2f)
36.1 degrees c
32.9 degrees c
31.3 degrees c
28.7 degrees c
26.6 degrees c
25.0 degrees c
24.1 degrees c
23.5 degrees c
22.5 degrees c
21.5 degrees c
20.8 degrees c
20.4 degrees c
18.7 degrees c
Intensity (counts)
Wavelength (nm)

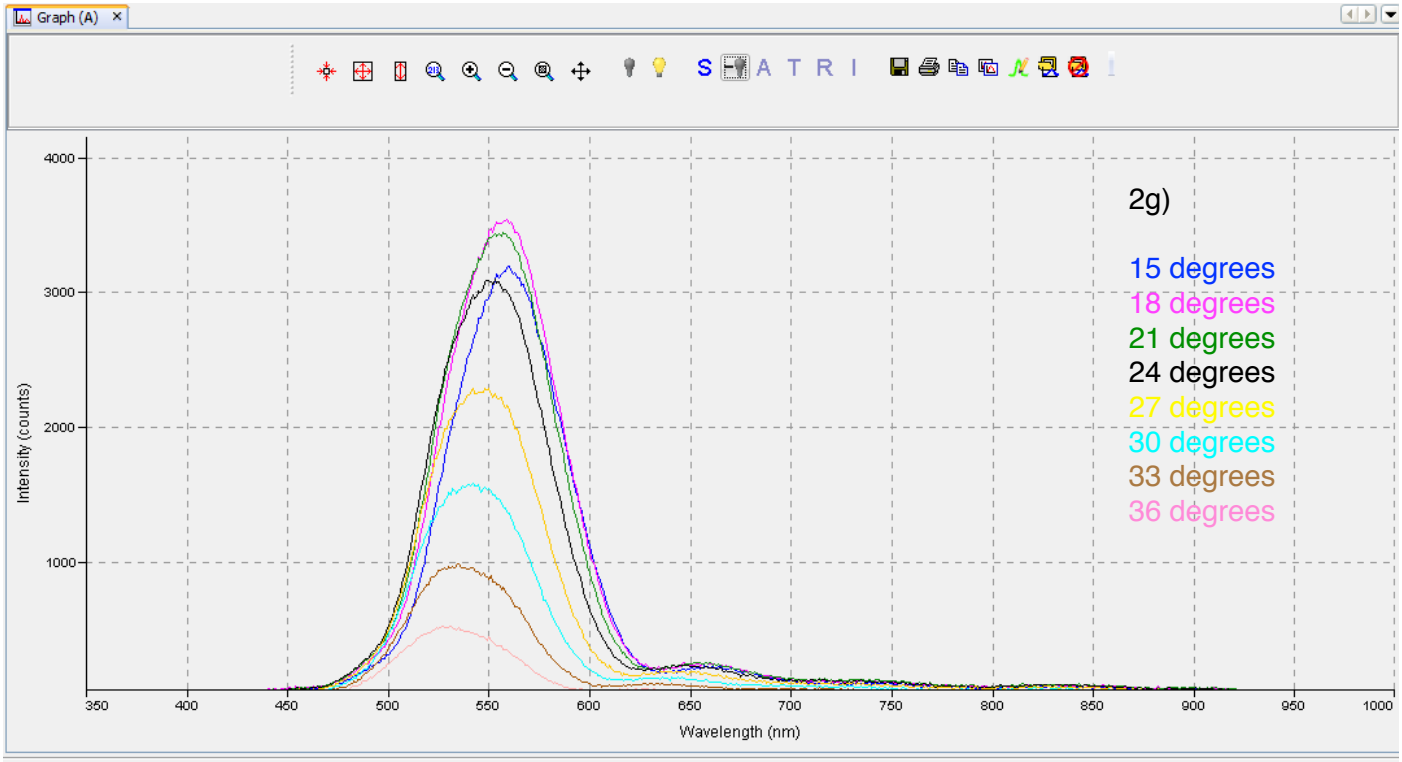
Graph (A)
S A T R I
2g)
15 degrees
18 degrees
21 degrees
24 degrees
27 degrees
30 degrees
33 degrees
36 degrees
Intensity (counts)
Wavelength (nm)
4000
3000
2000
1000
350
400
450
500
550
600
650
700
750
800
850
900
950
1000

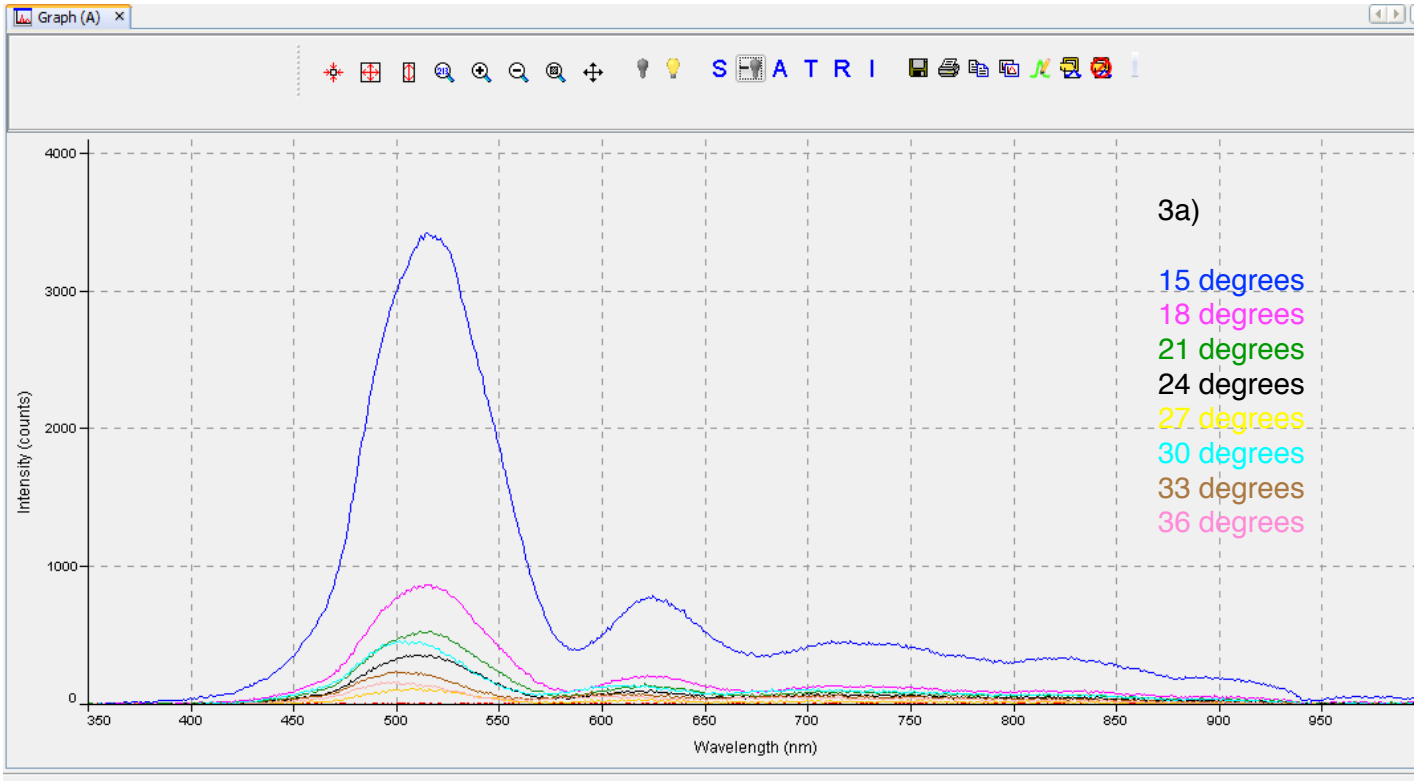
Graph (A)
S A T R I
3a)
15 degrees
18 degrees
21 degrees
24 degrees
27 degrees
30 degrees
33 degrees
36 degrees
Intensity (counts)
Wavelength (nm)
4000
3000
2000
1000
0
350
400
450
500
550
600
650
700
750
800
850
900
950

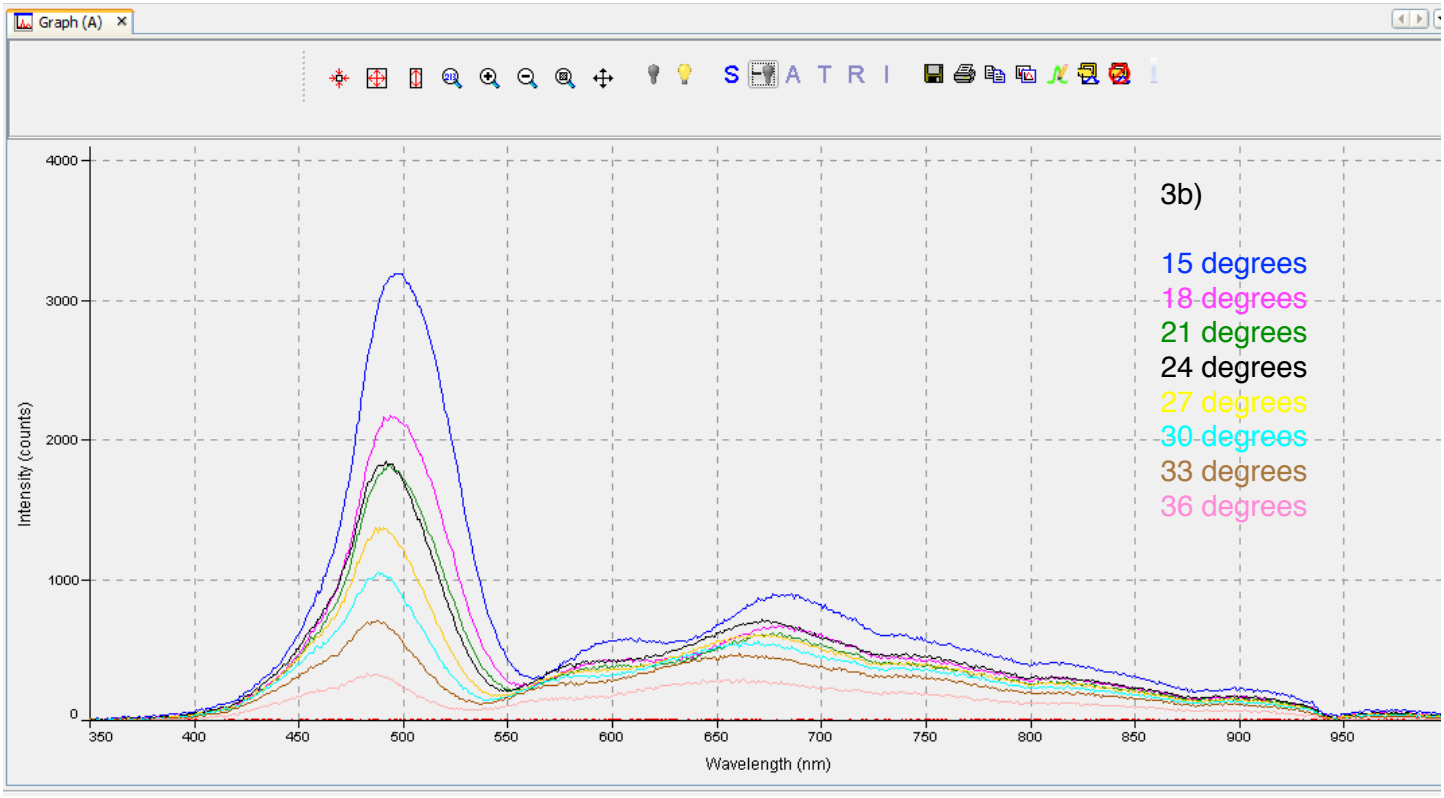
Graph (A)
3b)
15 degrees
18 degrees
21 degrees
24 degrees
27 degrees
30 degrees
33 degrees
36 degrees
Intensity (counts)
Wavelength (nm)
0
1000
2000
3000
4000
350
400
450
500
550
600
650
700
750
800
850
900
950

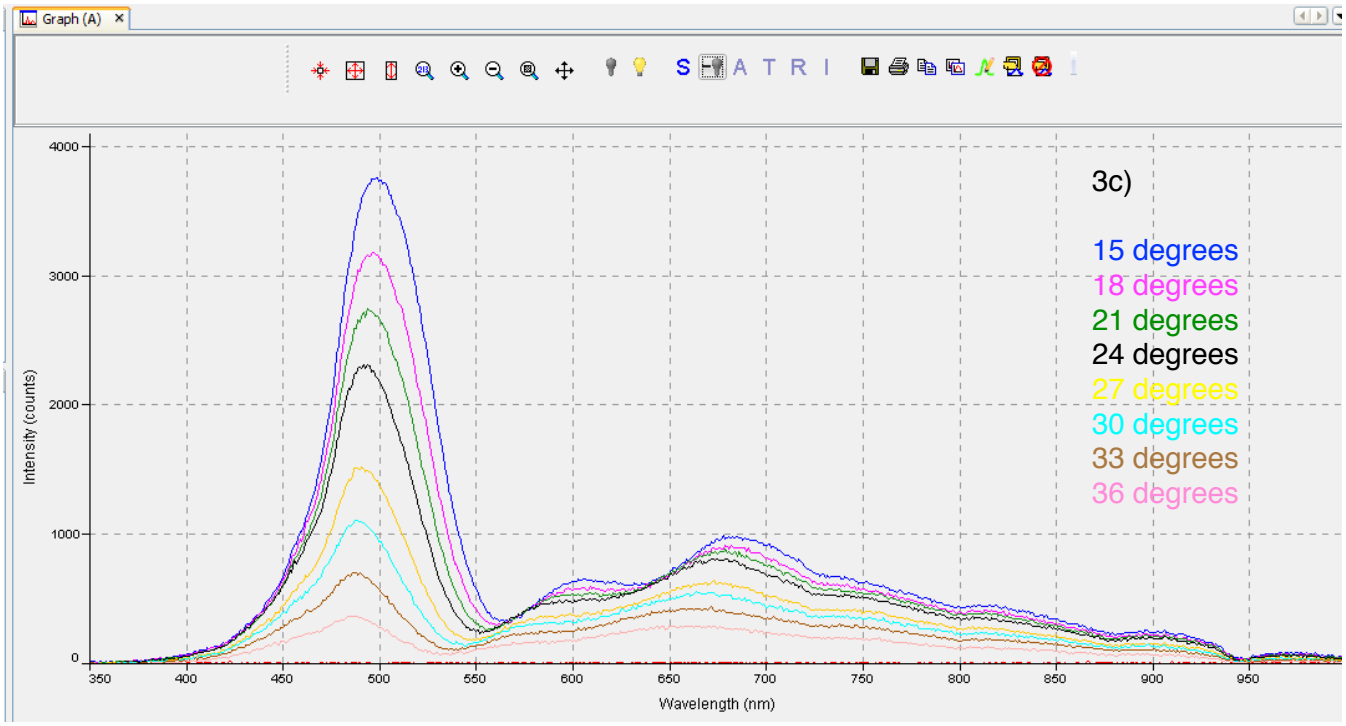
Graph (A)
3c)
15 degrees
18 degrees
21 degrees
24 degrees
27 degrees
30 degrees
33 degrees
36 degrees
Intensity (counts)
Wavelength (nm)
0
1000
2000
3000
4000
350
400
450
500
550
600
650
700
750
800
850
900
950

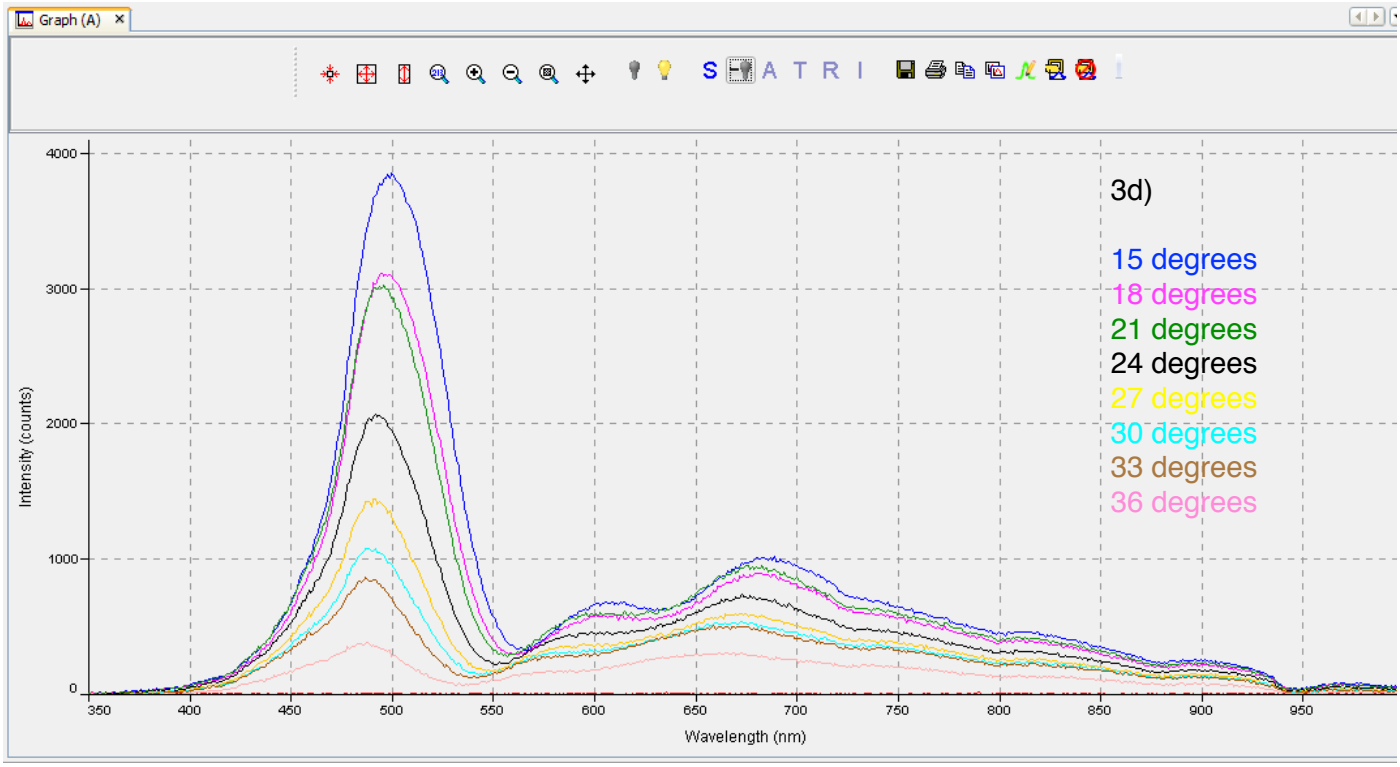
Graph (A)
S A T R I
3d)
15 degrees
18 degrees
21 degrees
24 degrees
27 degrees
30 degrees
33 degrees
36 degrees
Intensity (counts)
Wavelength (nm)
0
1000
2000
3000
4000
350
400
450
500
550
600
650
700
750
800
850
900
950

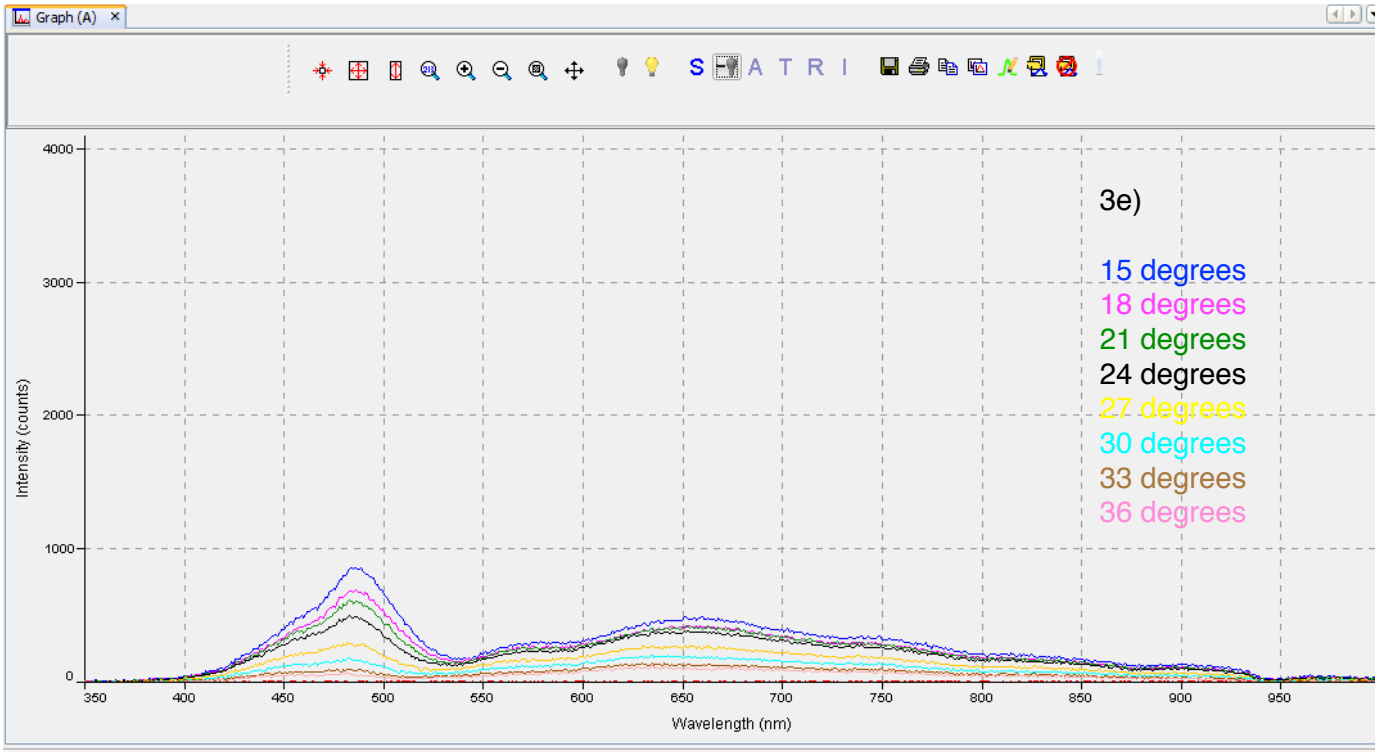
Graph (A)
S A T R I
3e)
15 degrees
18 degrees
21 degrees
24 degrees
27 degrees
30 degrees
33 degrees
36 degrees
Intensity (counts)
Wavelength (nm)
0
1000
2000
3000
4000
350
400
450
500
550
600
650
700
750
800
850
900
950

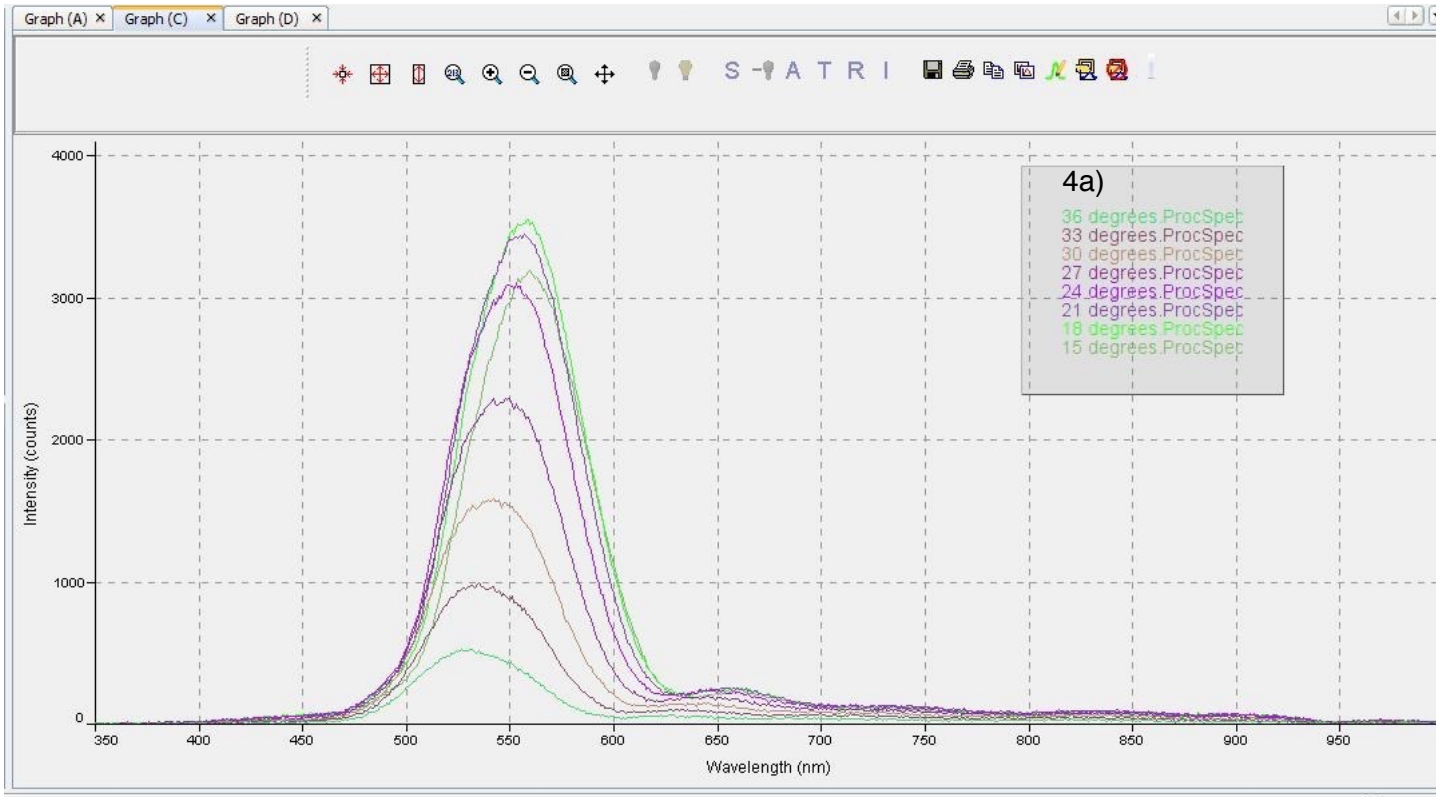
Graph (A)
Graph (C)
Graph (D)
4a)
36 degrees.ProcSpec
33 degrees.ProcSpec
30 degrees.ProcSpec
27 degrees.ProcSpec
24 degrees.ProcSpec
21 degrees.ProcSpec
18 degrees.ProcSpec
15 degrees.ProcSpec
Intensity (counts)
Wavelength (nm)

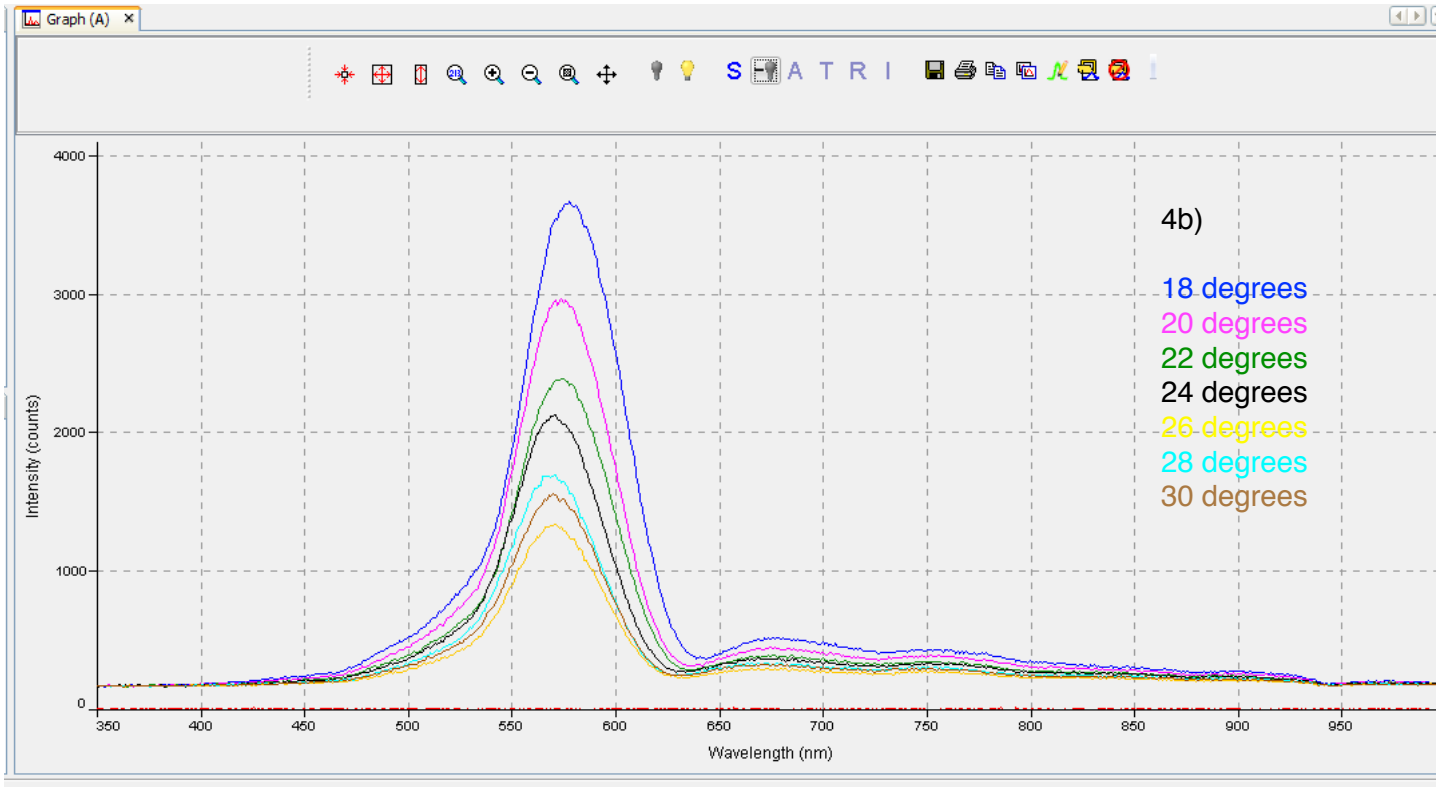
Graph (A)
4b)
18 degrees
20 degrees
22 degrees
24 degrees
26 degrees
28 degrees
30 degrees
Intensity (counts)
Wavelength (nm)

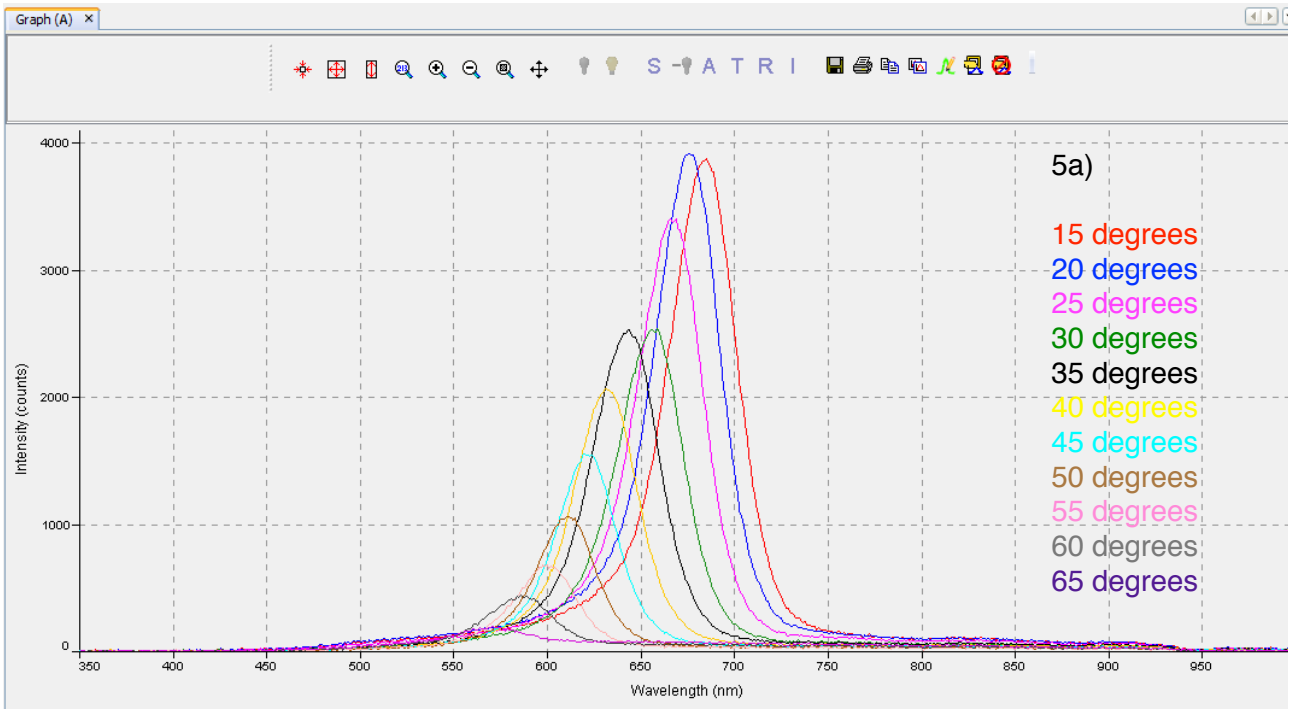
Graph (A)
5a)
15 degrees
20 degrees
25 degrees
30 degrees
35 degrees
40 degrees
45 degrees
50 degrees
55 degrees
60 degrees
65 degrees
Intensity (counts)
Wavelength (nm)

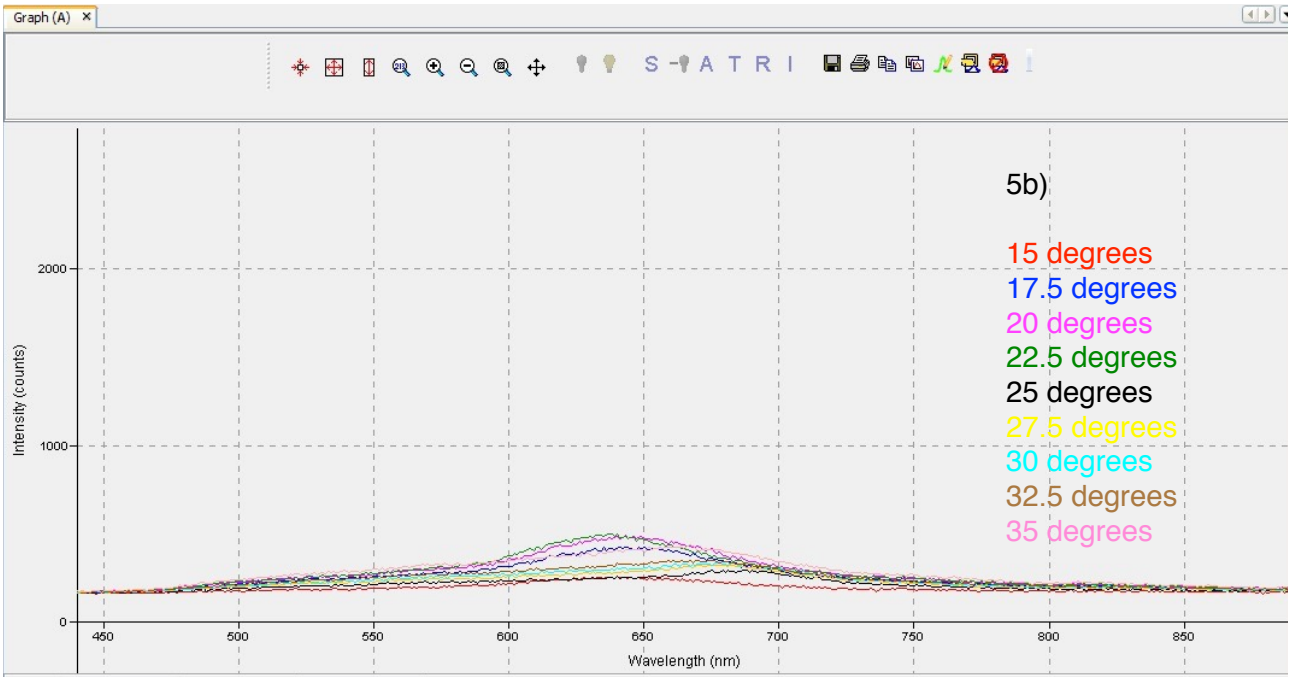
Graph (A)
5b)
15 degrees
17.5 degrees
20 degrees
22.5 degrees
25 degrees
27.5 degrees
30 degrees
32.5 degrees
35 degrees
Intensity (counts)
Wavelength (nm)

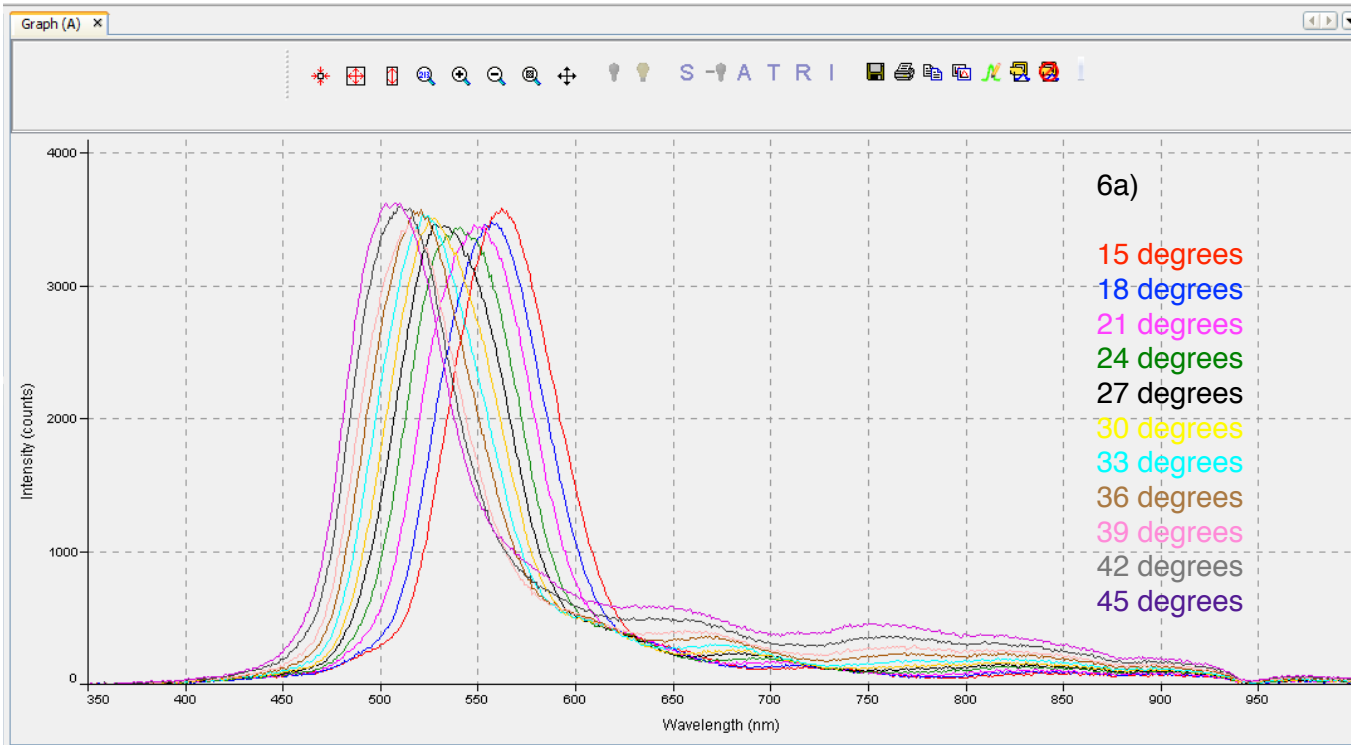
Graph (A)
6a)
15 degrees
18 degrees
21 degrees
24 degrees
27 degrees
30 degrees
33 degrees
36 degrees
39 degrees
42 degrees
45 degrees
Intensity (counts)
Wavelength (nm)
0
1000
2000
3000
4000
350
400
450
500
550
600
650
700
750
800
850
900
950

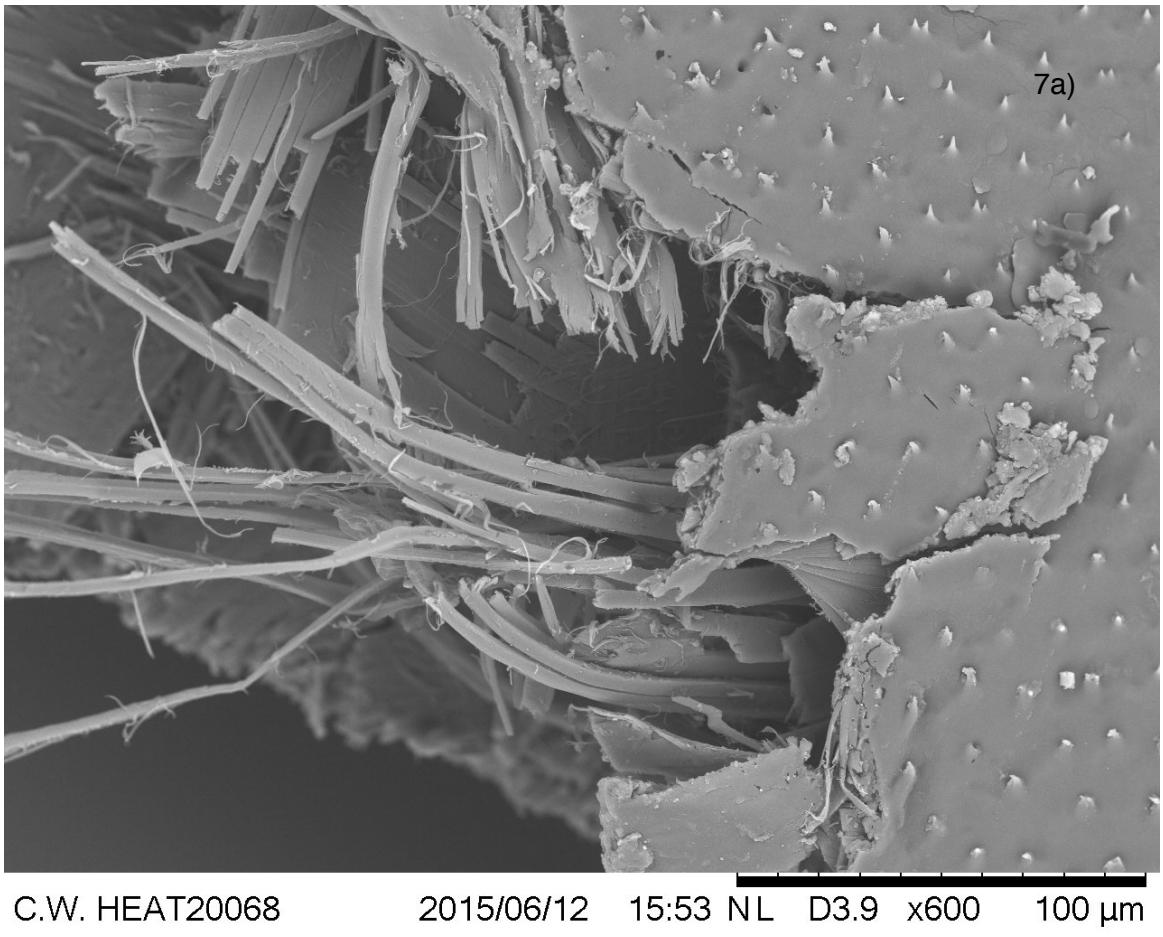
7a)
C.W. HEAT20068
2015/06/12
15:53 NL
D3.9
x600
100 µm

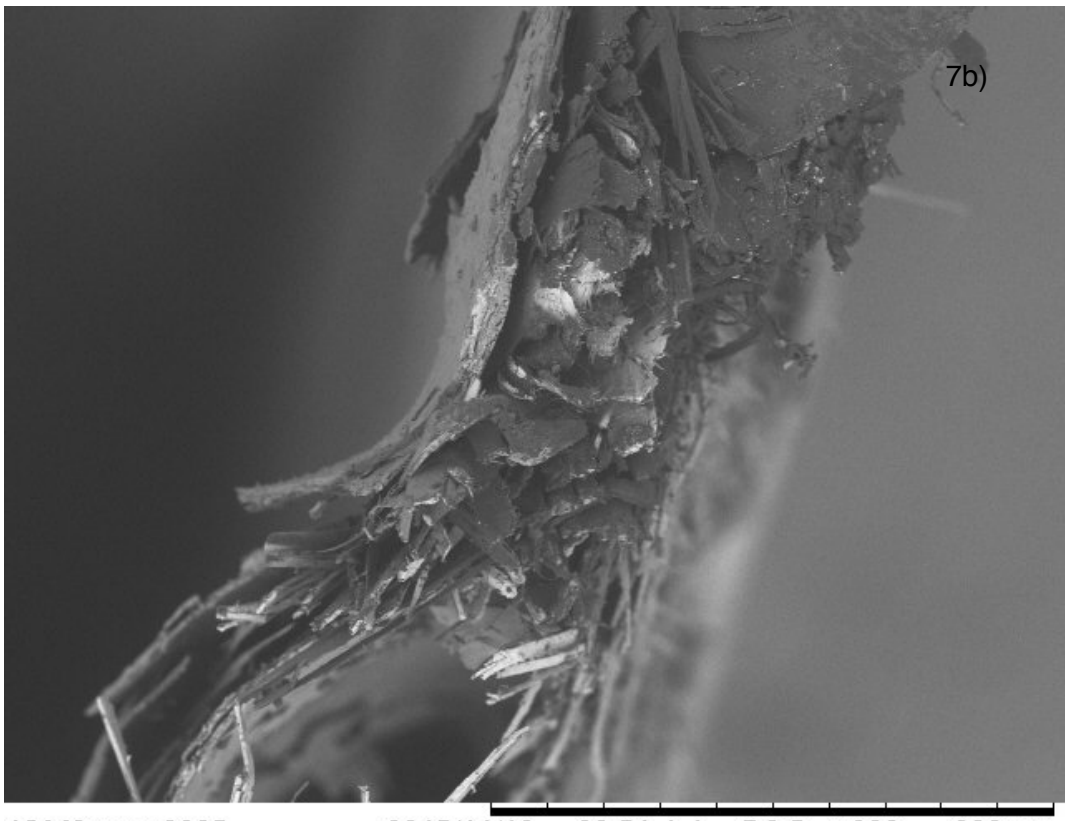
7b)
IOM3_ymc0005 2015/11/13 09:51 I L D3.5 x300 300 µm
15kV *15000

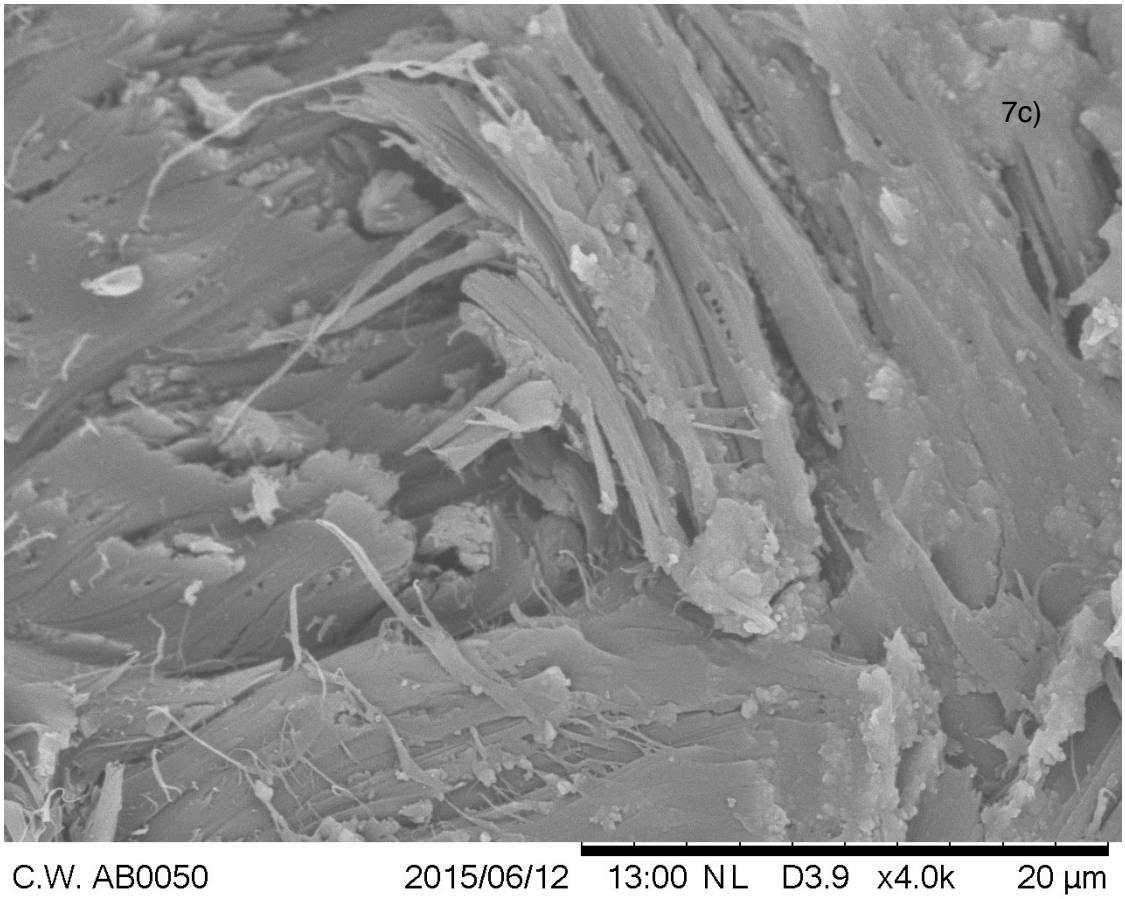
7c)
C.W. AB0050 2015/06/12 13:00 N L D3.9 x4.0k 20 µm

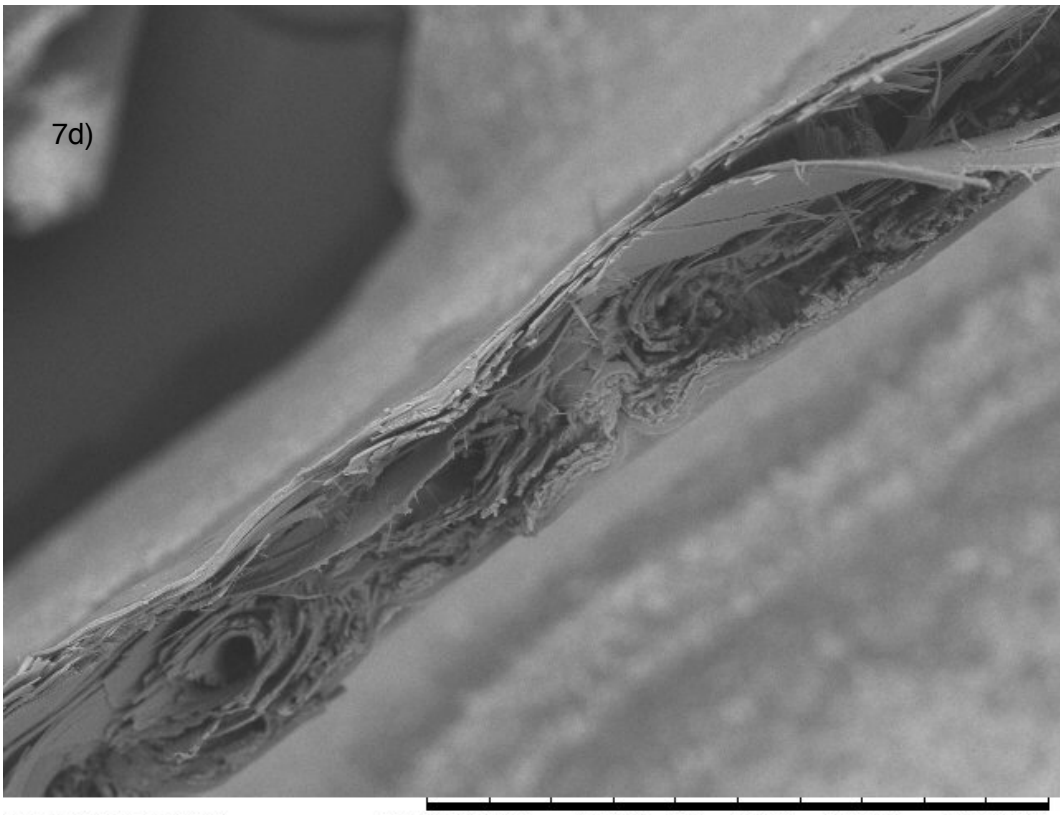
7d)
IOM3_ymc0038 2015/11/13 11:41 AL D7.4 x200 500 µm
15kV *15000

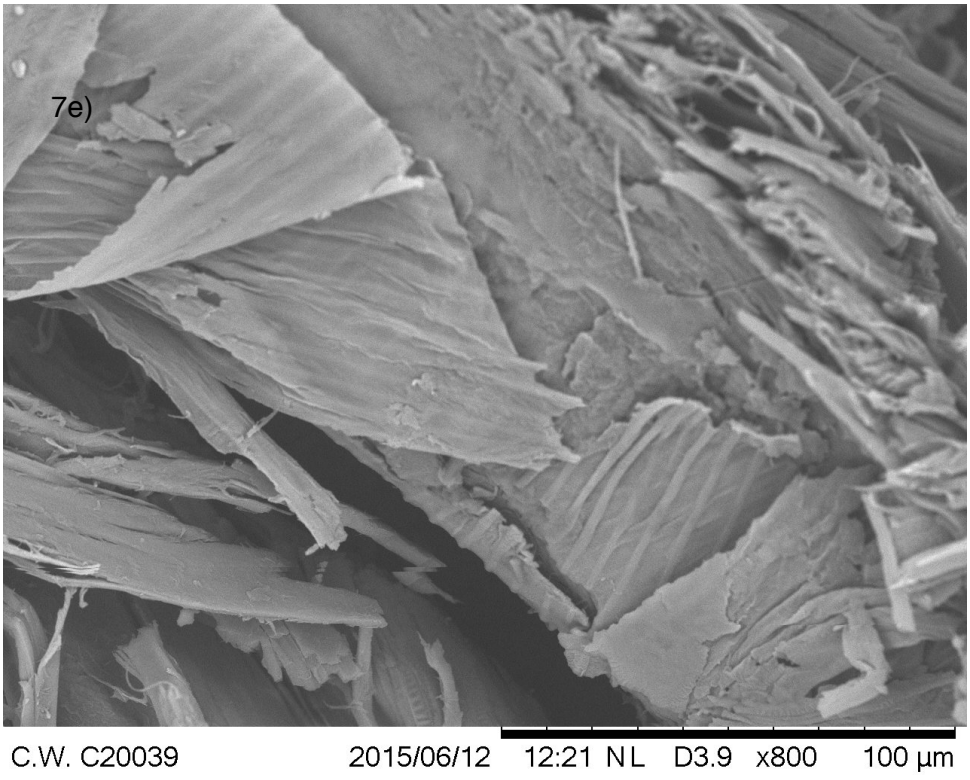
7e)
C.W. C20039 2015/06/12 12:21 NL D3.9 x800 100 µm

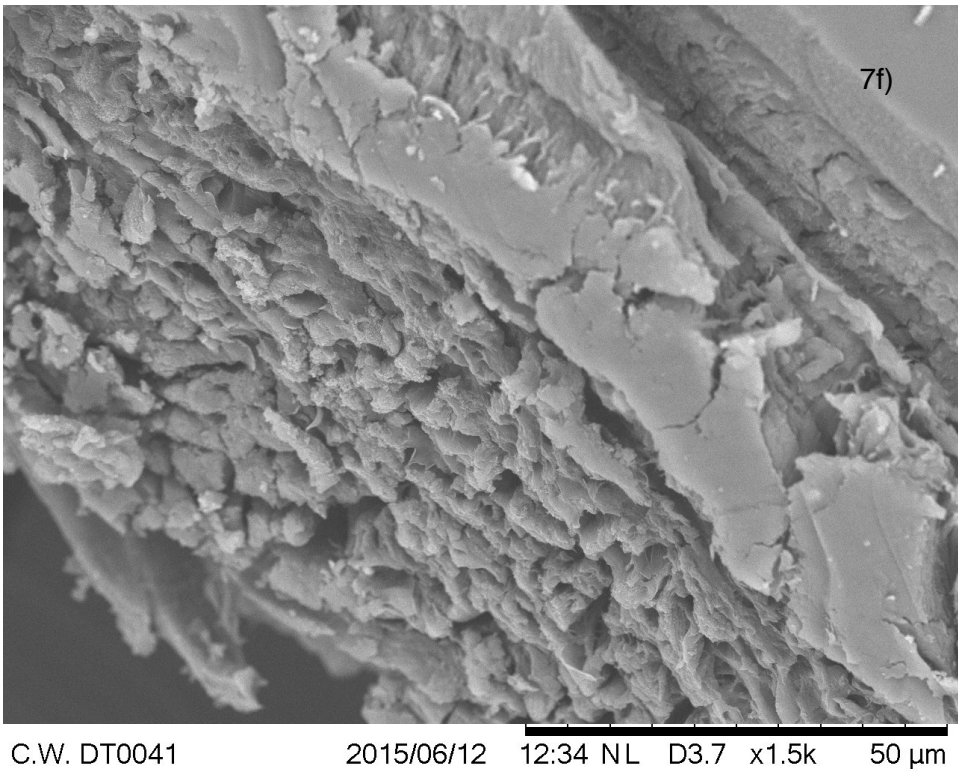
7f)
C.W. DT0041 2015/06/12 12:34 NL D3.7 x1.5k 50 µm

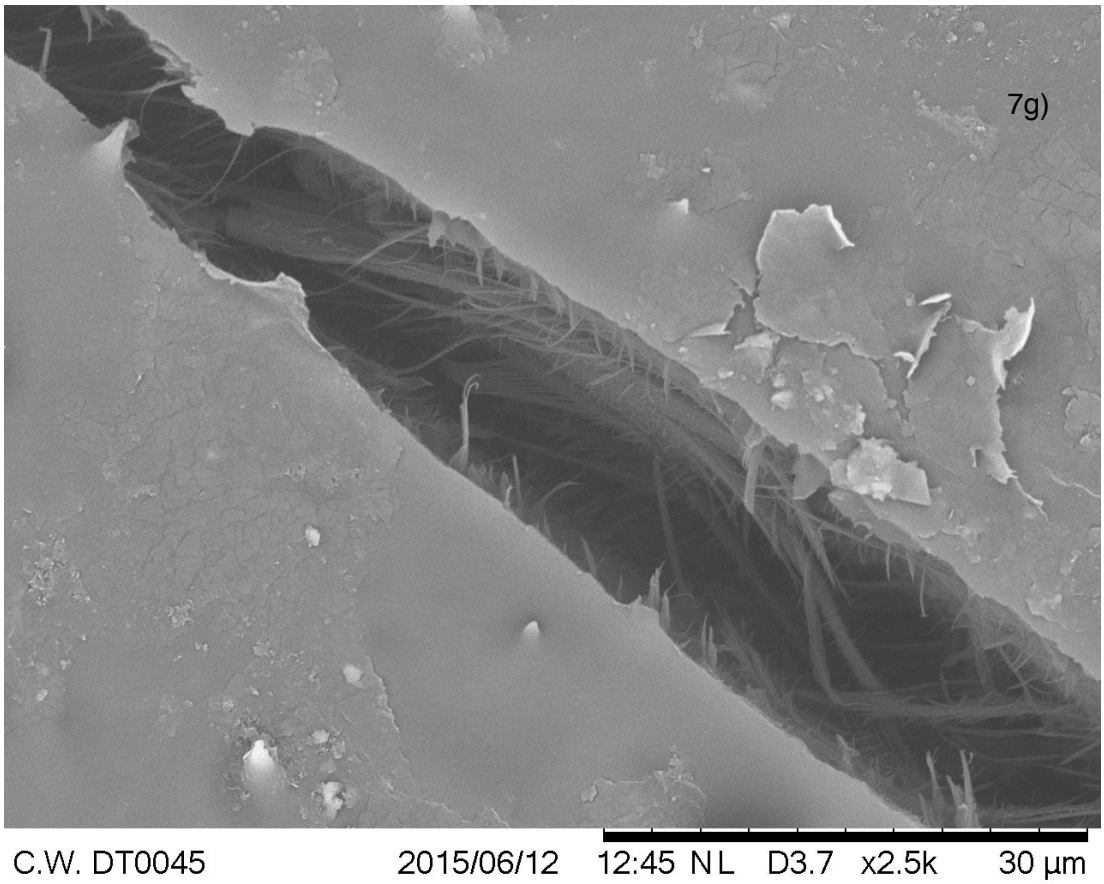
7g)
C.W. DT0045 2015/06/12 12:45 NL D3.7 x2.5k 30 µm

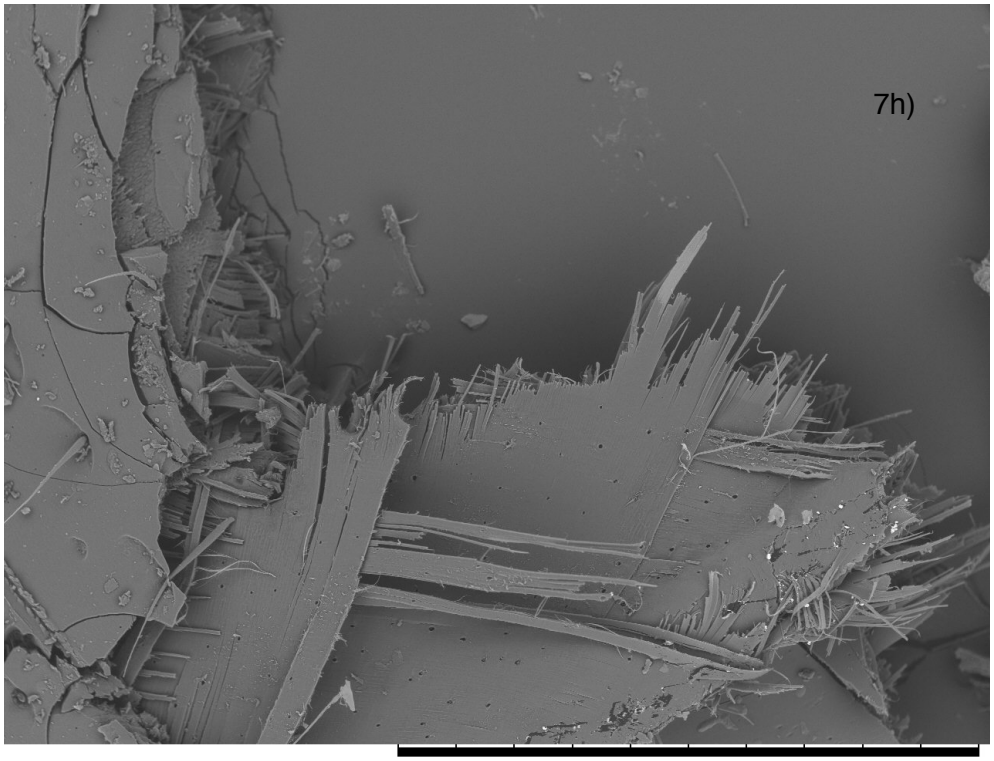
7h)
T.F.20057
2015/06/12 15:24 N L D3.8 x100 1 mm


7i)
2nd-right0028
2015/06/12 11:40 I L D3.9 x300 300 µm

6. Discussion:

6.1 Analysis:

The spectra above show the wavelength (on the x-axis) and intensity (on the y-axis) of the light reflected from the elytron. The light source shines white light on the elytron and some wavelengths are absorbed by the chitin layers but some are reflected. These reflected wavelengths are picked up by the receiver and the spectrometer processes them. The peak wavelength on the spectra shows the most significant wavelength that is reflected. The intensity of light is the same as the brightness of light.

Figure 1a) shows that the peak wavelength for red card remains at around 625 nm at all angles, confirming that the card is not iridescent. It supports the fact that the card is red because red wavelengths range from 620 nm to 750 nm. However the intensity decreases as the angle of incidence increases. This is probably because as the angle increases, the light has to refract more and therefore it loses power which means that the brightness of the reflected light decreases. Similarly, 1b) also confirms that the green card is not iridescent. The peak wavelength remains at around 525 nm and the range of wavelengths for green light is 495 nm to 570 nm. However, there is another peak at around 750 nm, which is very near the boundary between visible light and infrared. This peak could represent the infrared light being reflected, or the red pigment that is mixed with blue to create the green card.

Figure 2g) shows that for the heat controlled *C. wallacei*, the peak wavelength falls from 560 to 530 nm and the intensity ranges from 500 to 3500 counts as the angle increases from 15 to 36 degrees. This means that at smaller angles, the beetle appears green and at greater angles it appears blue-green. 2a) shows that the peak shifts from around 515 to 525 nm as the temperature cools down from 25.0 to 17.1 degrees celsius, at an angle of incidence of 15 degrees. Therefore the amount of red shift is very small and heat causes a lower peak wavelength to be reflected. The intensity remains at around 600 counts while calling takes place. The peak wavelength of figure 2b) shifts from around 490 to 500 nm as the temperature cools down from 32.1 to 18.1 degrees celsius. Therefore the wavelength shifts by the same amount as that of 15 degrees, although the temperature change is greater. Also, the peak wavelength is lower than that at 15 degrees because the elytron starts off at a higher temperature. Unlike 2a) the intensity varies from 900 to 1200 counts. Figure 2c) is the graph for angle of incidence of 21 degrees. The peak wavelength shifts from around 490 to 495 nm as the temperature cools from 46.5 to 23.6 degrees celsius. This shift is even smaller than the previous shifts, even though the temperature change is significantly greater. The starting peak wavelength is also the same as the previous although the temperature starts more than 10 degrees celsius higher. The intensity varies from 3400 to 4000 counts. At this point I would have expected the peak wavelength shift to be proportional to the temperature decrease and the peak wavelength to decrease regularly as the temperature was increased. The result for 2c) may not fit this pattern because the elytron may not have been completely perpendicular to the normal of the light source and receiver. 2d) shows that for 24 degrees, the peak shifts from around 630 to 640 nm as the temperature falls from 39.9 to 20.1 degrees celsius, however the peak is significantly less intense so it is difficult to tell which wavelength corresponds to the peak. These results might be anomalies because the *C. wallacei* is relatively constant in colour (it has no distinctive stripes or patterns) so I would have expected the peak to be lower than 500 nm because for the control, as the angle increases the peak decreases and also heat causes the wavelength to decrease. For 27 degrees, 2e)

shows that the peak wavelength shifts from 670 to 680 nm as the temperature falls from 49.8 to 19.0 degrees celsius and the intensity varies from 500 to 1500 counts. Again, I would have expected a larger shift due to the large change in temperature and high start temperature. Unfortunately, the peak wavelength is not clear enough from the graph of 2f) as the intensities are too close together.

The next set of results support the first few results of the previous set of data. 3a) demonstrates that for 0 hours after heating, the peak wavelength decreases from around 520 to 500 nm as the angle of incidence increases from 15 to 36 degrees. The shift is not as large as that of the control, but the pattern of iridescence is the same; blue shift still takes place even after heating. Overall, the peak wavelength is lower for the heated elytron than the control, which supports the results of 2a), 2b) and 2c), as these peak wavelengths were also lower than the peak of the control. 3b) shows that 1 hour after heating, the peak decreases from around 495 to 485 nm as the angle increases from 15 to 36 degrees. This result is not what I expected, because the peak wavelength is still decreasing even though the elytron is cooling down. I would have expected the overall wavelengths to increase back to the values of the control because after 1 hour the elytron cooled down to its original temperature. 2 hours after heating, the peak wavelength decreases from around 500 to 485 nm as the angle increases from 15 to 36 degrees (3c)). 3d) shows that at 3 hours after heating, the peak wavelength shifts by the same amount as the previous graph. After 3 hours, the peak wavelength remained this way which suggests that the heating caused a permanent and therefore irreversible change in the colour reflected from the elytron. However, I expected the change to be temporary. The permanent change might have been caused by heating the elytron for too long or at a temperature that denatured the colour. 3e) is the graph of the elytron after heating it for a second time. The peak wavelength starts at 490 nm but it is difficult to tell how much it shifts as the other peaks are too flat. The intensities are also significantly lower. Therefore the colour reflected did not change much, which suggests that once the elytron has been put under extreme heat stress, any other environmental changes will not affect it anymore because it has been denatured. Overall, despite the colour change, the results show that the elytron still possesses iridescent properties, because as the angle of incidence increases blue shift of the peak wavelength occurs.

7a) and 7c) show the differences between the top surfaces of the control and heated elytron. Firstly, the layers in 7a) appear to be cross-layered, and the fibres are not facing the same direction. The edge is very rough due to the fact that the sample was ripped because it was very difficult to cut precisely due to the fibres. The surface of the layers in 7c) appears rougher than the surface in 7a), but 7c) is more than 6 times as magnified as 7a). Therefore although I cannot be sure, it is probable that the layers are rougher because any moisture that was between them would have evaporated. This is an effect of heat, on the nanostructure of the elytron. 7b) and 7d) demonstrate the differences between the side edges of the control and heated elytron. 7b) shows that the edge is very rough and jagged. I used a programme called ImageJ to measure the approximate thickness of the layers in both pictures. The average thickness in 7b) was 4.050 um, whereas the thickness in 7d) was around 6.772 um. Therefore the layers become thicker after heat is applied. This may be because the layers collapsed and therefore appear thicker as they are closer together.

After the elytron was heated for the first time, it turned completely purple but started to return to its original colour. After the second time, the purple colour remained. Purple/violet wavelengths are in the 400 to 450 nm range. The graphs, especially 2b), 2c), 3b) and 3e) show that the peaks are close to being violet, but are blue. For all the heated results, there was a second peak at around 670 nm, which is the wavelength of red light. this may be because the purple light split into two components: red wavelengths and blue wavelengths. The peak wavelength might have decreased

after heating, because the moisture between the layers decreased, so they collapsed and caused only red and blue wavelengths to be reflected and not absorbed. Therefore for the results above, I would conclude that they support my first and third hypotheses.

4a) shows the results of the NaOH control. The peak wavelength decreases from 560 to 530 nm and the intensity varies from 500 to 3500 counts as the angle increases from 15 to 36 degrees. This is the same pattern as the heat control. 4b) shows that after the elytron has been treated with NaOH and dried with anhydrous calcium chloride, the peak wavelength decreases from 580 to 570 nm and the intensity varies from 1300 to 3700 counts as the angle of incidence increases from 18 to 30 degrees. This means that after the treatment the peak wavelength increased, which partly disagrees with my hypothesis. Dehydration may cause the peak to increase, because the water from the chitin layers will evaporate and therefore the difference in refractive index between the layers and surrounding air will be lower (and the chitin layers will become less optically dense). Therefore most incident light of low wavelengths are absorbed but red wavelengths are reflected. However the elytron is still iridescent because as the angle of incidence increases the peak wavelength of reflected light decreases, which agrees with the second part of my hypothesis.

7e) shows the ripped edge of a sample of an NaOH controlled elytron. The direction of the fibres are visible and the edge is very rough. 7f) shows that after treatment with NaOH, the layers appear to be clumped together which may be a result of the moisture evaporating from them.

The results of the *T. flammea flammea* NaOH control demonstrate that the peak wavelength decreases significantly from 680 to 570 nm a the angle increases from 15 to 65 degrees (Figure 5a)). The intensity varies from 200 to 3900 counts. The peak shifts by approximately 11 degrees for each 5 degrees angle change and you can see from the graph that these shifts are regular. This supports my second hypothesis. The peak wavelength is generally higher (in the red range) because the nanostructure in the centre of the elytron is different to the nanostructure of the rest of the elytron. Different nanostructure produce different iridescent effects and therefore a different colour is reflected. Figure 5b) shows that after dehydration, the peak wavelength is 40 nm lower. It decreases from 640 to 630 nm as the angle increases from 15 to 22.5 degrees and then suddenly the wavelength increases to 690 nm and decreases again to 660 nm from 25 to 35 degrees. These inconsistent results may be a result of the elytron not being completely perpendicular to the normal between the light source and receiver. Therefore between 15 and 22.5 degrees a mixture of green and red wavelengths may have been reflected, whereas from 25 degrees more red wavelengths than green wavelengths may have been reflected. However these results may just be anomalous.

7h) and 7i) show the differences between the controlled and dehydrated *T. flammea flammea*. The fibres in 7i) are significantly rougher and more strands are loose. 7h) shows a more rigid nanostructure. Dehydration causes the moisture in the nanostructure to evaporate and the absence of moisture causes a rougher surface for the chitin layers.

Finally, figure 6a) shows the graph for the boiled *C. wallacei* elytron. The peak wavelength decreases from 570 to 510 nm as the angle increases from 15 to 45 degrees. The wavelength shifts equally each time the angle increases by 3 degrees. The intensity range is very small; it ranges from around 3400 to 3500 counts. Therefore the peak is slightly higher than that of the control, which supports my last hypothesis. The elytron is still iridescent because the reflected colour changes as the angle of incidence is increased, which also supports the hypothesis. Boiling causes the wavelength to increase, because increased moisture between the layers causes the difference in

refractive index between the layers and air decrease and the optical thickness of the layers may increase. Therefore higher wavelengths will be reflected.

6.2 Reflection:

I was very lucky to be able to use all of the equipment that was required for the experiments and the SEM. having access to the spectrophotometer allowed me to record the precise wavelengths and therefore colours of the reflected light. The only limitation was that I could not find a way to retain the heat for the heated elytron experiment so that the temperature remained constant but high, while the angle was increased.
After completing this project, I have learnt how to manage my time and work towards deadlines more efficiently. Being able to work on a high level, scientific research project has been very enjoyable and the EPQ has enabled me to summarise all of the experiments and results. Also, it has given me the chance to try and reason why and how these effects have changed the iridescent properties of the beetles that were investigated. It has enabled me to gain confidence in obtaining results using the goniometer setup, spectrophotometer and the software SpectraSuite which has improved my computing skills. I have learnt about the uses of iridescence in the natural world and I would like to study this further.
Next, I would like to investigate the effects of freezing the elytron to find out if the change in state causes a significant change in colour, and how this changes the nanostructure of the beetle.

7. Bibliography:

Figure 1: *Iridescent properties of a soap bubble*- www.wikinut.com
Figure 2: www.superstrate.net
Figure 3: www.voer.edu.vn
Figure 4: *Two waves that are coherent*- CGP AS level physics guide
Figure 5: www.math.ubc.ca
Figure 6: www.math.ubc.ca
Figure 7: www.webexhibits.com
Figure 8: Seago *et al.* (2009), *(a) Simple diagram of multilayer cuticular reflector, (b) TEM cross section of cuticular reflector of Cicindela scutellaris.*
Figure 9: Seago *et al.* (2009), (*a*) *Pachyrrhynchus congestus pavonius*- SEM of crystal structure from scale interior (from Welch & Vigneron 2007), (*b*) SEM of the interior structure of *Prosopocerus lactator.*
Figure 10: Seago *et al.* (2009), *(a) Schematic of cuticular grating, (b) SEM of diffraction grating, Sphaeridiinae gen. sp. (Hydrophilidae), and (c) Sphaeridiinae gen. sp., habitus view with zero, first, second and third spectral orders labelled.*

Barnard, A.S. et al. (2008) *Nature's Nanostructures*

Glover, B.J. and Whitney, H.M. (2010) *Structural colour and iridescence in plants: the poorly studied relations of pigment colour,* Annals of Botany www.aob.oxfordjournals.org.

Seago A.E, Brady P, Vigneron J. and Schultz, T.D. (2009) *Gold bugs and beyond: a review of iridescence and structural colour mechanisms in beetles (Coleoptera)* The Royal Society

Vukusic, P. and Stavenga, D.G. (2009) *Physical methods for investigating structural colours in biological systems* The Royal Society